Response to Comments of Reviewer #1

(comments in *italics*)

Manuscript number: EGUSPHERE-2023-2393

Title: Weakened aerosol-radiation interaction exacerbating ozone pollution in eastern China since China's clean air actions

This paper mainly investigated the impacts of aerosol-photolysis interaction (API) and aerosol-radiation feedback (ARF) on the surface ozone concentrations under the background of China's clean air action (rapid anthropogenic emission reductions from 2013 to 2017).

The effects of API on ozone concentrations are not a new finding since I have found several previous studies already addressed it (Gao et al., 2022; Liu and Wang, 2020). However, I have not found any previous studies focused on the effects of ARF on ozone concentrations. Furthermore, the authors used the IPR methodology to investigate the contribution to O_3 concentration variation from four processes (VMIX, CHEM, ADVH, ADVZ). In conclusion, I consider this paper valuable for publication, even if it has some limitations (as shown below). (1) The absence of SOA formation and heterogeneous reactions in their simulations could be a limitation of this study; even the authors have sufficiently acknowledged this. (2) Some parts/aspects are poorly elucidated, making it hard for me to understand. A major revision is needed before it can be published in ACP.

Response:

Thanks to the reviewer for the valuable comments and suggestions which are very helpful for us to improve our manuscript. We have revised the manuscript carefully, as described in our point-to-point responses to the comments.

The major innovation of this study is that **it is the first time** to quantify the response of aerosol-radiation interaction to anthropogenic emission reduction from 2013 to 2017, with the mainly focus on the contribution to changed O_3 concentrations over eastern China both in summer and winter.

According to the reviewer's comments, **another three** widely used chemical mechanisms, i.e., RADM2-MADE/SORGAM (RADM2 gas-phase chemistry coupled with MADE/SORGAM aerosol module), CBMZ-MADE/SORGAM (CBMZ gas-phase chemistry coupled with MADE/SORGAM aerosol module), and MOZART-MOSAIC (MOZART gas-phase chemistry coupled with MOSAIC aerosol module), that include SOA formation are also applied to test the impact of aerosol-radiation interaction (ARI) on O_3 with and without SOA.

Comparing the simulation results of the three additional mechanisms, the simulated $PM_{2.5}$ from MOZART-MOSAIC are closer to the actual observation. Analyzing the summer/winter MDA8 O_3 reductions due to ARI by the mechanism used in our manuscript (i.e., CBMZ-MOSAIC) and MOZART-MOSAIC, **similar results are quantified** (1.32 ppb *vs.* 1.85 ppb for summer, and 1.96 ppb *vs.* 1.60 ppb for winter). Therefore, although the CBMZ-MOSAIC used in this paper does not take into account the formation of SOA and its associated effects, the aerosol radiative effect on O_3 concentration is consistent with the results when the SOA simulation mechanism is considered.

The impacts of aerosol heterogeneous reactions on O_3 have not been considered in this

manuscript due to the **uncertainty and inconsistency** of the heterogeneous uptake shown in previous observation and simulation studies (Liu and Wang., 2020b; Tan et al., 2020; Shao et al., 2021). Shao et al. (2021) summarized that different heterogeneous uptake on the aerosol surface applied in the model simulation (e.g., 0.20 *vs.* 0.08) would cause significant deviations in simulated ozone concentrations (e.g., O_3 increased by 6% *vs.* O_3 increased by 2.5%). Therefore, the uncertainty in the heterogeneous uptake value used in the numerical simulation will finally amplify the deviation in model results.

According to the reviewer's comments about some poorly elucidated parts, such as ΔO_3_ΔARF_EMI. We have **detailedly described** in our point-to-point responses as shown below, and related descriptions have also been added in the revised manuscript.

Specific comments:

1. *In my opinion, SOAs account for a substantial portion of total aerosols. Typically, in your research, the lack of consideration of SOA can truly affect the reliability of the results (the authors also mentioned that $PM_{2.5}$ is underestimated in your model). I highly recommend the authors include SOA formation in their model.*

Response:

Thanks to the reviewer for the valuable comments and suggestions. The CBMZ gas-phase chemistry coupled with MOSAIC aerosol module (CBMZ-MOSAIC for short) used in this study does not include secondary organic aerosol (SOA), then we applied three additional chemical mechanisms that consider SOA, namely, RADM2 gas-phase chemistry coupled with MADE/SORGAM aerosol module (RADM2-MADE/SORGAM for short), CBMZ gas-phase chemistry coupled with MADE/SORGAM aerosol module (CBMZ-MADE/SORGAM for short), and MOZART gas-phase chemistry coupled with MOSAIC aerosol module (MOZART-MOSAIC for short), to test the impact of ARI on O_3 with and without SOA for the scenario of BASE_17E17M.

Figures R1 shows the temporal variations of observed and simulated $PM_{2.5}$ and O_3 concentrations over eastern China for the three additional chemical mechanisms. Comparing with the observed $PM_{2.5}$ (O_3) concentrations, the MOZART-MOSAIC showed the best performance in December 2017, with the R of 0.73 (0.79) and NMB of -18.7% (-20.5%). Therefore, we further used this mechanism to simulate the air pollutant concentrations during the period of June 2017. As shown in Fig. R1 (a4, b4), the temporal variations of observed $PM_{2.5}$ (O_3) can be well captured by this mechanism with R of 0.56 (0.91) and NMB of -1.7% (-20.3%).

Finally, we investigated the effect of aerosol-radiation interaction (ARI) on O_3 from the results of CBMZ-MOSAIC (this mechanism applied in this manuscript which does not include SOA) and MOZART-MOSAIC (this mechanism includes SOA and performs the best simulation results comparing with RADM2-MADE/SORGAM and CBMZ-MADE/SORGAM). As shown in Fig. R2, summer (winter) MDA8 O_3 is significantly reduced over eastern China, ARI reduces the surface MDA8 O_3 concentrations by 1.32 (1.96) ppb and 1.85 (1.60) ppb by CBMZ-MOSAIC and MOZART-MOSAIC, respectively. The O_3 reductions are of comparable magnitude in these two schemes. Therefore, we can conclude that although the CBMZ-MOSAIC applied in this manuscript does not take into account the formation of SOA and its associated effects, the aerosol radiative effects on O_3 concentrations not only in the pattern of spatial-temporal distribution but also in the order of magnitude are consistent with the results when the SOA simulation mechanism is considered.

As shown in Fig. R3, the mean SOA simulated by RADM2-MADE/SORGAM, CBMZ-

MADE/SORGAM, and MOZART-MOSAIC are 0.29, 0.45 and 0.94 μg m^{-3}, accounting for 3.4%, 3.8%, and 4.4% of $PM_{2.5}$ concentrations in winter 2017, respectively. From Fig. R4, the mean SOA simulated from MOZART-MOSAIC is 0.90 μg m^{-3}, account for 9.1% of $PM_{2.5}$ in summer 2017. Model simulated SOA concentrations are generally underestimated in most current chemical transport models (Zhang et al., 2015; Zhao et al., 2015). The low SOA concentrations simulated by the model can be explained by low emissions of biogenic and anthropogenic VOCs (key precursors of SOA), but a thorough investigation of this underestimation is outside the scope of this manuscript and it will be discussed in our future work. (**Page 18-19, Line 497-536**)

According to the reviewer's suggestion, we have added Figs. R1-R4 in the revised support information. **(Page 13-16 in supporting information)**

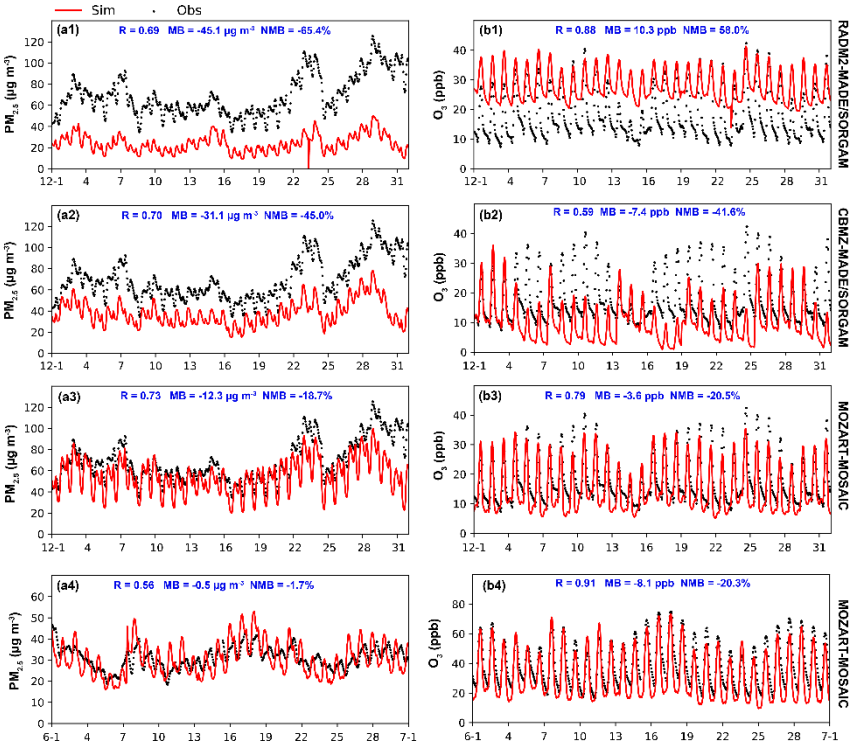

Figure R1. Time series of observed (black dots) and simulated (red lines) hourly **(a1-a4)** $PM_{2.5}$ and **(b1-b4)** O_3 concentrations averaged over the whole observation sites in eastern China during summer and winter 2017. **(a1, b1)** Simulated $PM_{2.5}$ and O_3 concentrations in winter 2017 by RADM2 gas-phase chemistry coupled with MADE/SORGAM aerosol module (RADM2-MADE/SORGAM). **(a2, b2)** Simulated $PM_{2.5}$ and O_3 concentrations in winter 2017 by CBMZ gas-phase chemistry coupled with MADE/SORGAM aerosol module (CBMZ-MADE/SORGAM). **(a3, b3)** Simulated $PM_{2.5}$ and O_3 concentrations in winter 2017 by MOZART gas-phase chemistry coupled with MOSAIC aerosol module (MOZART-MOSAIC). **(a4, b4)** is the same as **(a3, b3)**, but for summer 2017. The calculated correlation coefficient (R), mean bias (MB), and normalized mean bias (NMB) are also shown.

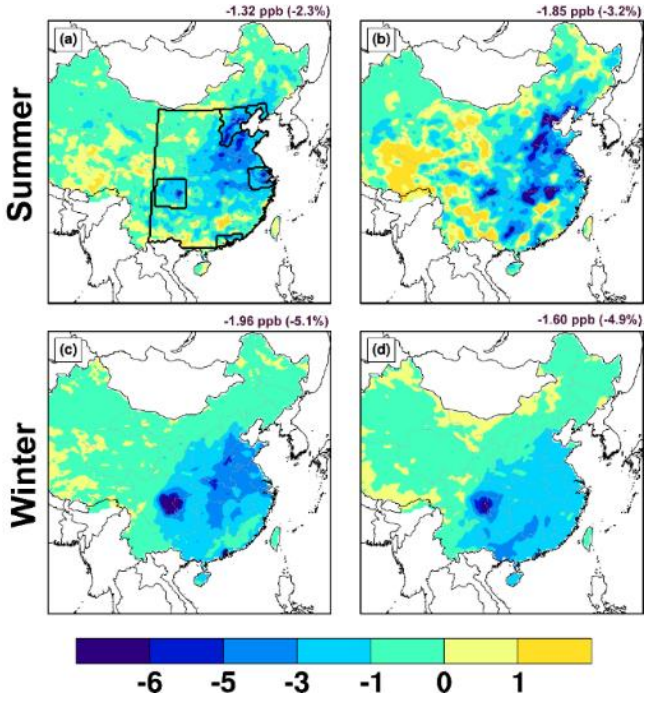

Figure R2. The effects of aerosol-radiation interaction on surface-layer MDA8 O_3 in summer (upper) and winter (bottom) 2017 calculated by **(a, c)** CBMZ-MOSAIC and **(b, d)** MOZART-MOSAIC mechanisms. The changes (percentage changes) averaged over China are also shown at the top of each panel.

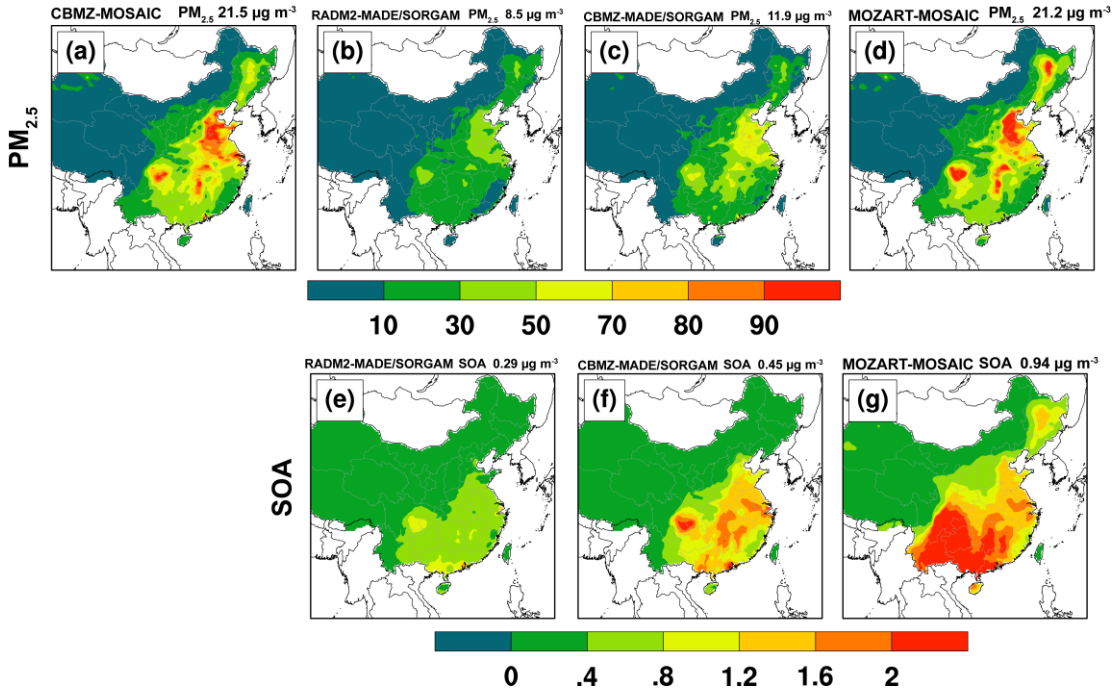

Figure R3. Spatial distributions of simulated mean $PM_{2.5}$ and SOA concentrations (μg m^{-3}) in winter 2017 by **(a)** CBMZ gas-phase chemistry coupled with MOSAIC aerosol module (CBMZ-MOSAIC), **(b, e)** RADM2 gas-phase chemistry coupled with MADE/SORGAM aerosol module (RADM2-MADE/SORGAM), **(c, f)** CBMZ gas-phase chemistry coupled with MADE/SORGAM aerosol module (CBMZ-MADE/SORGAM), and **(d, g)** MOZART gas-phase chemistry coupled with MOSAIC aerosol module (MOZART-MOSAIC). The calculated pollutant concentrations averaged over China are also shown at the top of each panel.

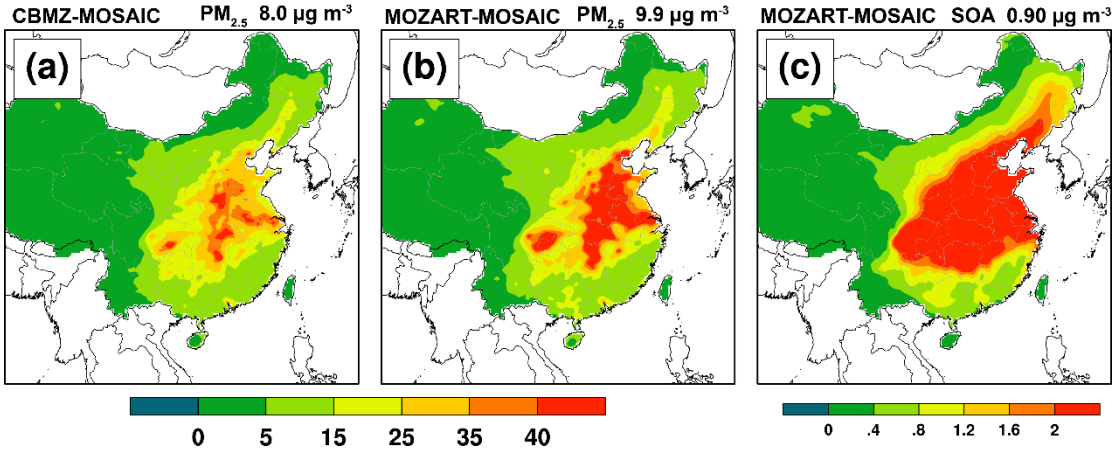

Figure R4. Spatial distributions of simulated mean $PM_{2.5}$ and SOA concentrations (μg m^{-3}) in summer 2017 by **(a)** CBMZ gas-phase chemistry coupled with MOSAIC aerosol module (CBMZ-MOSAIC), (b, c) MOZART gas-phase chemistry coupled with MOSAIC aerosol module (MOZART-MOSAIC). The calculated pollutant concentrations averaged over China are also shown at the top of each panel.

2. *Similarly, as the significant impacts of heterogeneous reactions on ozone concentrations mentioned by previous studies (Lou et al., 2014; Liu and Wang, 2020), I would expect the authors to include heterogeneous reactions in their models. If the authors have specific reasons for not including heterogeneous reactions in their models, those reasons need to be stated in the paper.*

Response:

In addition to the impacts of aerosol-radiation interaction (ARI), aerosols can also affect the concentrations of O_3 by heterogeneous chemistry (HET). Liu and Wang. (2020b) found that the rapid decrease of $PM_{2.5}$ was a major contributor for the summer O_3 increase through weakening the heterogeneous uptake of hydroperoxy radical (HO_2). However, Tan et al. (2020) launched a field campaign in North China Plain (NCP) and proposed a contradicting opinion about the importance of the impact of HET on O_3. These inconsistent conclusions generated from field observations and numerical simulations are mainly originated from the different values of heterogeneous uptake they used. Tan et al. (2020) pointed out that the heterogeneous uptake of HO_2 on aerosol surface was 0.08 ($\gamma_{HO2} = 0.08$) over NCP, which is smaller than the values ($\gamma_{HO2} = 0.2$) used in model simulations (Li et al., 2019; Liu and Wang., 2020). As shown in Fig. R5, Shao et al. (2021) found controversial results by using the different heterogeneous uptake of HO_2. When $\gamma_{HO2} = 0.2$ was used in the chemical model, the reduced heterogeneous uptake of HO_2 due to the decrease in aerosol caused the maximum O_3 increased by about 6% from 2013 to 2016, which is close to the results of Li et al. (2019) (~ 7%). When $\gamma_{HO2} = 0.08$ was used, the reduced heterogeneous uptake of HO_2 due to the decrease in aerosol led to maximum O_3 increased by only 2.5% from 2013 to 2016. Therefore, significant deviations in the model results would result from the use of different heterogeneous uptake on the aerosol surface.

Furthermore, previous laboratory studies indicate that the uptake coefficient varies widely from 0.003 to 0.5 with a strong dependence on the concentration of transition metal ions such as Cu(II) and Fe(II) in the aerosol (Zou et al., 2019). Taketani et al. (2009) reported that the uptake coefficient of HO_2 (γ_{HO2}) on seawater particles depends on relative humidity (RH), with γ_{HO2} values of 0.10 ±

0.03, 0.11 ± 0.02 and 0.10 ± 0.03 at 35%, 50% and 75% RH, respectively. Lakey et al. (2015) also found that a large humidity dependence was observed for HO_2 uptake onto humic acid aerosols. The HO_2 uptake coefficient increased from 0.007 ± 0.002 to 0.06 ± 0.01 between 32 and 76% RH for the Acros organics humic acid, and from 0.043 ± 0.009 to 0.09 ± 0.03 between 33 and 75% RH for the Leonardite humic acid. This strong dependence on aerosol composition and RH implies that a single assumed value for heterogeneous uptake used in numerical simulation may cause large uncertainty. In addition, our manuscript devoted to quantifying the effects of ARI on O_3, rather than the impacts of heterogeneous reactions on O_3. Due to the reasons listed above, we did not consider the effect of heterogeneous reactions on O_3 temporarily in the manuscript.

Thanks for the reviewer's suggestion, and we will consider the impacts of heterogeneous reaction in our future works. A discussion about the impacts of heterogeneous reaction has been added in the revised manuscript as follows:

"The impacts of aerosol heterogeneous reactions (HET) on O_3 have not been considered in this manuscript due to the uncertainty and inconsistency of the heterogeneous uptake shown in previous observation and simulation studies (Liu and Wang., 2020b; Tan et al., 2020; Shao et al., 2021). Liu and Wang. (2020b) found that the rapid decrease of $PM_{2.5}$ was the primary contributor for the summer O_3 increase through weakening the heterogeneous uptake of hydroperoxy radical (HO_2). However, Tan et al. (2020) launched a field campaign in NCP and proposed a contradicting opinion about the importance of the impact of HET on O_3. Shao et al. (2021) summarized that different heterogeneous uptake on the aerosol surface applied in the model simulation (e.g., 0.20 *vs.* 0.08) would cause significant deviations in simulated ozone concentrations (e.g., O_3 increased by 6% *vs.* O_3 increased by 2.5%). Previous laboratory studies indicate that the dependence of the uptake coefficient on aerosol composition and RH means that a single assumed value for heterogeneous uptake used in numerical simulations can lead to large uncertainties (Lakey et al., 2015; Taketani et al., 2009; Zou et al., 2019). Therefore, the uncertainty in the heterogeneous uptake value used in the numerical simulation will finally amplify the deviation in model results. Meanwhile, our manuscript devoted to quantifying the effects of ARI on O_3, rather than the impacts of heterogeneous reactions on O_3. The absence of heterogeneous chemistry on aerosol surface may result in underestimation of the effect of aerosol on O_3, which will be considered in our future work." (**Page 19-20, Line 537-556)**

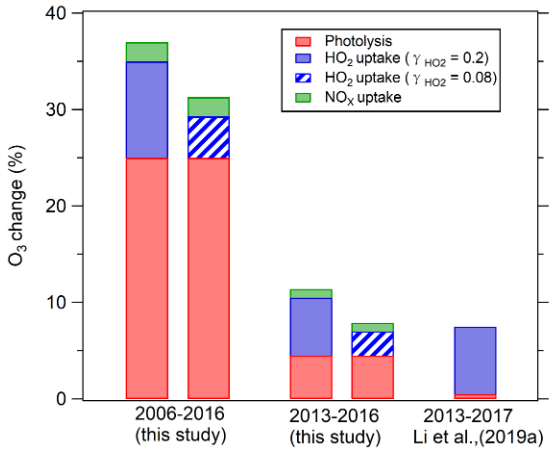

Figure R5. O_3 change due to the decrease in $PM_{2.5}$ during 2006-2016 and during 2013-2016 in the study of Shao et al., (2021) and during 2013-2017 in the study of Li et al., (2019a). This picture is from Shao et al., (2021).

3. *L160, you mentioned you fixed the meteorological field to the year 2013, can you explain how to achieve this? Can I understand that all *17M cases have exactly the same meteorological fields throughout 2017 simulation? However, I don't think all *17M cases should have the same meteorological fields, because you cannot investigate deltaO3_deltaARF_EMI if the meteorological fields are fixed in different cases. This needs to be explained more clearly in your paper.*

Response:

Thanks for your comments. ΔO_3_ΔARF_EMI represents the impacts of weakened aerosol-radiation feedback (ΔARF) due to decreased anthropogenic emission (EMI) on O_3 concentrations (ΔO_3). In order to quantify the impacts caused by the decreased EMI from 2013 to 2017, the impacts of changed meteorological variables should be removed by fixing the meteorological fields in year 2017 in sensitivity experiments, such as NOAPI_13E17M, NOALL_13E17M, NOAPI_17E17M and NOALL_17E17M (13E17M means anthropogenic emissions are from the year of 2013 and meteorological fields are from the year of 2017, more details can be found in Figure 1 in the revised manuscript).

For example, the differences between NOAPI_13E17M and NOALL_13E17M reflect the impact of ARF at the condition of 13E17M (the result is denoted as ΔO_3_ARF_{13E} for short), and the differences of NOAPI_17E17M and NOALL_17E17M show the impact of ARF at the condition of 17E17M (the result is denoted as ΔO3_ARF_{17E} for short), so the differences between ΔO3_ARF_{17E} and ΔO3_ARF_{13E} finally present the impact of weakened aerosol-radiation feedback due to decreased anthropogenic emission from 2013 to 2017 on O_3 concentrations.

For the summer simulations and the winter simulation in the year of 2013 or in the year of 2017, we use the June and December meteorological fields for the corresponding year.

The same method has been widely used in many other studies, which mainly focus on the impacts of weakened aerosol-radiation interactions on air pollutants in China (Li et al. 2019; Zhou et al., 2019; Hong et al. 2020; Liu and Wang. 2020b; Zhu et al. 2021; Shao et al. 2021).

According to the reviewer's suggestion, we have added this information in the revised manuscript. (**Page 7-8, Line 175-214**)

4. *L23-L25, you mentioned API and ARF. However, the API and ARF terminology is so abstract, making it hard for people to understand. It would help if you mentioned that API is related to the change in photolysis rates and ARF is related to the change of meteorological fields in your abstract.*

Response:

Thanks for your suggestion, we have added this information in the revised manuscript as follows: **"**Here we apply a coupled meteorology-chemistry model (WRF-Chem) to quantify the responses of aerosol-radiation interaction (ARI), including aerosol-photolysis interaction (API) related to photolysis rate change and aerosol-radiation feedback (ARF) related to meteorological fields change, to anthropogenic emission reductions from 2013 to 2017, and their contributions to O_3 increases over eastern China in summer and winter.**"** (**Page 2, Line 24-26**)

5. *L58, I think chemical species like CO and CH_4 can also lead to the formation of O_3.*

Response:

According to the reviewer's suggestion, we have changed the sentence in the revised

manuscript as follows: "As a secondary air pollutant, troposphere O_3 can be produced by nitrogen oxides (NO_x = NO + NO_2), carbon monoxide (CO), methane (CH_4) and volatile organic compounds (VOCs) in the presence of solar radiation through photochemical reactions (Atkinson, 2000; Seinfeld and Pandis, 2006)." (**Page 3, Line 60**)

6. *L57-L62 The causal relationship between the following two sentences is not clear. As a secondary air pollutant, troposphere O_3 can be produced by nitrogen oxides (NO_x = NO + NO_2) and volatile organic compounds (VOCs) in the presence of solar radiation through photochemical reactions (Atkinson, 2000; Seinfeld and Pandis, 2006). - > Consequently, the concentration of O_3 is closely related to changes in meteorological conditions and anthropogenic emissions (Wang et al., 2019; Liu and Wang, 2020a,b; Shu et al., 2020). "solar radiation" is not directly related to "meteorological conditions", try to revise those sentences to make them more logical.*

Response:

Thanks for your suggestion. we have changed the sentence in the revised manuscript as follows: "The concentration of O_3 in the troposphere is influenced by changes in meteorological conditions (e.g., high temperature and low relative humidity) and its precursors emissions (e.g., NOx and VOCs) (Wang et al., 2019; Liu and Wang, 2020a,b; Shu et al., 2020). Most precursors are from anthropogenic sources, and some precursors can come from natural sources, such as biogenic VOCs and soil and lightning NOx." (**Page 3, Line 62-67**)

7. *2.1 Model configuration: I recommend using a chart (like Table 1 in https://www.sciencedirect.com/science/article/pii/S1352231020307378) to summarize the model configuration.*

Response:

Thanks to the reviewer's comments, the model configuration is summarized in Table R1. We have added Table R1 in the revised supporting information. (**Table S1**)

Table R1. WRF-Chem model configurations with main physical and chemical schemes adopted in this study.

Model set-up	**Values**
Domain	East Asia
Study period	June and December 2017
Domain size	167 × 167
Domain center	34 °N, 108 °E
Horizontal resolution	27 km × 27 km
Vertical resolution	32 eta levels up to 50 hPa
Meteorological boundary and initial conditions	NCEP 1°×1° reanalysis data
Chemical initial and boundary conditions	CAM-Chem output
Physical options	**Adopted scheme**
Microphysics scheme	Lin (Purdue) scheme
Cumulus scheme	Grell 3D ensemble scheme
Boundary layer scheme	Yonsei University PBL scheme
Surface layer scheme	Monin-Obukhov surface scheme
Land-surface scheme	Unified Noah land-surface model

Longwave radiation scheme	RRTMG
Shortwave radiation scheme	RRTMG
Chemical options	**Adopted scheme**
Gas phase chemistry	CBMZ
Aerosols	MOSAIC
Photolysis	Fast-J
Biogenic emissions	MEGAN
Anthropogenic emissions	MEIC

8. *L125-L127, have you applied meteorological nudging? See above, I am not sure how you fix the meteorological fields to 2013 or 2017 when running the model.*

Response:

This work is done without nudging because only one domain is designed in our manuscript. If the nudging is turned on in only one domain simulation, the simulated meteorological field can not truly reflect the influence of the aerosol-radiation interaction feedback.

When using the 2013 (2017) FNL meteorological field data, it means that the meteorological field are from the year of 2013 (2017). For example, BASE_17E17M means that the meteorological field and anthropogenic emission are from the year of 2017. BASE_13E13M means that the meteorological field and anthropogenic emission are from the year of 2013.

9. *L151, you mentioned the biogenic emissions are calculated online by MEGAN. Have you coupled the MEGAN model with WRF-Chem dynamically? Please ascertain whether the biogenic emissions are calculated online or offline by MEGAN.*

Response:

Thanks to the reviewer's comments. In this work, we set "bio_emiss_opt = 3" in the WRF-Chem model, which represents the biogenic emissions can be calculated online by the coupled MEGAN module based upon the simulated meteorological variables (e.g., temperature, solar radiation) and underlying static data (e.g., leaf area index, plant types).

10. *L166, can you explain which aerosol optical properties are turned to zero?*

Response:

Following Qiu et al. (2017), the aerosol radiation interactions were turned off by removing the mass of aerosol species from the calculation of aerosol optical properties. Then, the aerosol optical properties such as aerosol optical depth (AOD), aerosol single scattering albedo (SSA), aerosol asymmetery factor (g) and aerosol backscatter coefficient were set to zero.

11. *L200-202, you mentioned "To avoid potential deviations caused by long-term model integration, each simulation is re-initialized every eight days". I was confused about why re-initialize the simulation every eight days can avoid potential deviations. What do you mean "potential deviations"? Can you explain this more?*

Response:

Thanks to the reviewer's comments. Lo et al. (2008) conducted three types of experiments for the entire year of 2000 to test model performance for different simulation durations: (1) continuous

integrations with a single initialization as usually done, namely, one year of uninterrupted simulation (WRFS), (2) consecutive integrations with re-initializations every 29 days (WRFM-30D), and (3) same as (2) but the model is reinitialized every 6 days (WRFM-7D). They found that the traditional continuous integration approach (WRFS) shows the worst performance. The model drifts from the forcing FNL reanalysis during the course of long integrations. It poorly simulates not only the forcing variables, (e.g., pressure, temperature, wind, and moisture), but also the model diagnostics variables (e.g., precipitation). Therefore, the simulation is re-initialized every eight days in this work, the same as the WRFM-7D, to avoid the deviation from forcing variables, (e.g., pressure, temperature, wind, and moisture) and model diagnostics variables (e.g., precipitation).

12. *L214-217 I feel confused about how many sites are operated by China National Environmental Monitoring Center (CNEMC)? You mentioned "1296 sites", does this number refer to the number of total sites of CNEMC or the number of sites chosen in your research? Moreover, are there really 1296 points (sites) on Figs. 2a and 2c?*

Response:

The CNEMC had 1484 observation sites in 2017. In this work, a single site with at least 500 actual observations during the simulated period are used for model evaluation, as we mentioned in the manuscript (**Page 9, Line 238-240**). Of course, Figs. 2a and 2c does have 1296 sites.

13. *Figure 2 shows the simulated results of which case? (BASE_17E17M?) You need to specify this point in L251 and Fig. 2.*

Response:

According to the reviewer's comment, we made it clear in Section 3 in the revised manuscript that the simulation results from the case of BASE_17E17M are used to evaluate the model performs (**Page 10, Line 264-266**).

14. *Why there are less points on Figs. 3a and 3d than Fig. 2? Please explain.*

Response:

Thanks to the reviewer's comments. The CNEMC installed only 450 sites in 2013, which grew to more than 1500 stations by 2020. In Fig. 3, only sites with continuous observations and individual site data greater than 500 were used to assess ozone trends. Thus, Fig. 3 has fewer points than Fig. 2.

15. *L221, if possible, I recommend explaining more about IPR in your paper.*

Response:

Thanks to the reviewer's suggestion, we have added this sentence in the revised manuscript as follows: "Process analysis techniques, i.e., integrated process rate (IPR) analysis, can be used in grid-based Eulerian models (e.g., WRF-Chem) to obtain contributions of each physical/chemical process to variations in pollutant concentrations. Eulerian models utilize the numerical technique of operator splitting to solve continuity equations for each species into several simple ordinary differential equations or partial differential equations that only contain the influence of one or two processes (Gipson, 1999).

In order to quantitatively elucidate individual contributions of physical and chemical processes

to O_3 concentration changes due to weakened ARI, the integrated process rate (IPR) methodology is applied in this study. IPR analysis is an advanced tool to evaluate the key process for O_3 concentration variation (Shu et al., 2016; Zhu et al., 2021; Yang et al., 2022). In this study, the IPR analysis tracks hourly (e.g., one time step) contribution to O_3 concentration variation from four main processes, including vertical mixing (VMIX), net chemical production (CHEM), horizontal advection (ADVH), and vertical advection (ADVZ). VMIX is initiated by turbulent process and closely related to PBL development, which influences O_3 vertical gradients. CHEM represents the net O_3 chemical production (chemical production minus chemical consumption). ADVH and ADVZ represent transport by winds. We define ADV as the sum of ADVH and ADVZ." (**Page 9-10, Line 245-262**)

16. *Table 2, how many sites are used for Table 2 (1296 sites?)?*

Response:

Thanks to the reviewer's comments. Table 2 contains 1296 sites, and we added this information to the revised manuscript (**Page 31, Line 811**).

17. *L284-285, you mentioned NOx-limited and VOCs-limited regions, I recommend that you could add a figure (based on your simulation results) like Fig. 5 in https://www.sciencedirect.com/science/article/pii/S1352231013000514 to your supplement, to show different O_3-sensitive regions on the map.*

Response:

The typical VOCs/NO_x ratio is calculated to classify sensitivity regimes and to indicate the possible O_3 responses to changes in VOCs and/or NO_x concentrations. O_3 production is VOC-limited if the ratio is less than 4, and it is NO_x-limited if the ratio is larger than 15 (Edson et al., 2017; Li et al., 2017). The ratio of VOCs/NO_x ranging around 4-15 indicates a transitional regime, where ozone is nearly equally sensitive to each species (Sillman, 1999). As shown in Fig R6, O_3 are mainly formed under the VOC-limited in winter and NO_x-limited and transitional regimes in eastern China, which is consistent with what our study mentioned.

According to the reviewer's suggestion, we have added Fig. R6 in the revised support information. **(Page 7 in supporting information)**

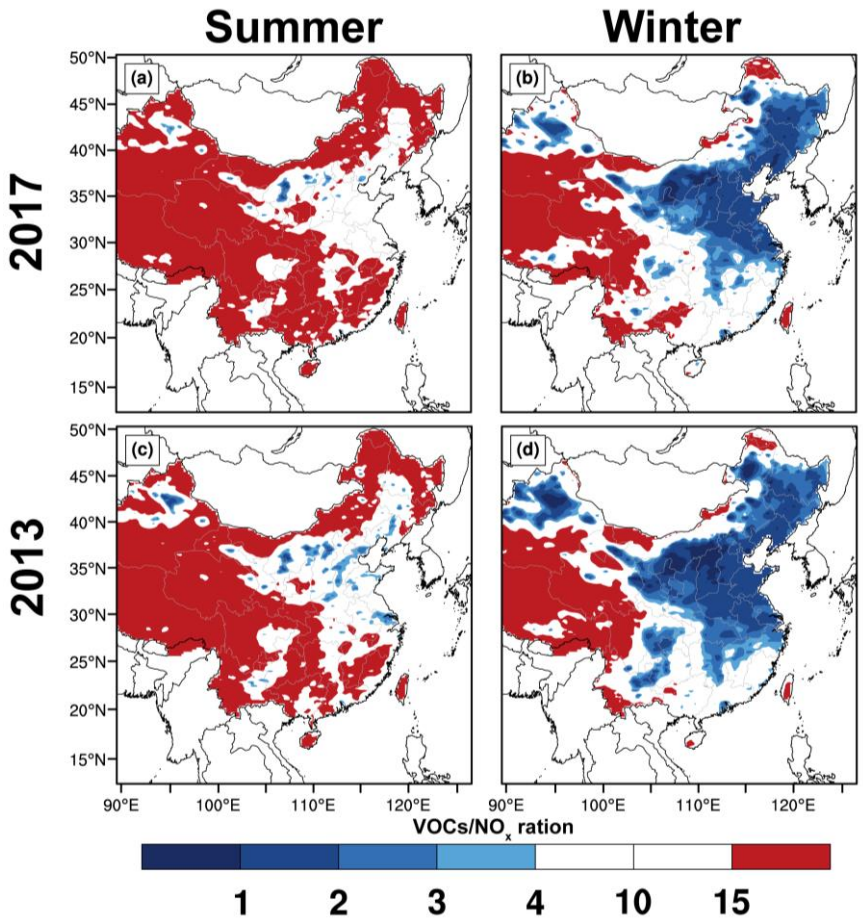

Figure R6. The ratios of VOCs/NO_x calculated from (a, b) BASE_17E17M, and (c, d) BASE_13E13M during the daytime (08:00-17:00 LST) from summer (left) and winter (right).

18. *L290-292, the meteorological effects are comparable or larger or smaller than emissions effects? This should be mentioned.*

Response:

From Figs. R7, compared with 2013, the meteorological conditions in the summer of 2017 promoted the generation of O_3 in the YRD region, but suppressed the generation of O_3 in the BTH, PRD and SCB regions. In PRD and SCB, the changes in MDA8 O_3 due to meteorology even have a greater impact than that by emission changes, which highlights the significant role of meteorology on summer O_3 variations during summer.

Thanks for reviewer's suggestion, we have added this information in the revised manuscript. **(Page 13, Line 343-349)**

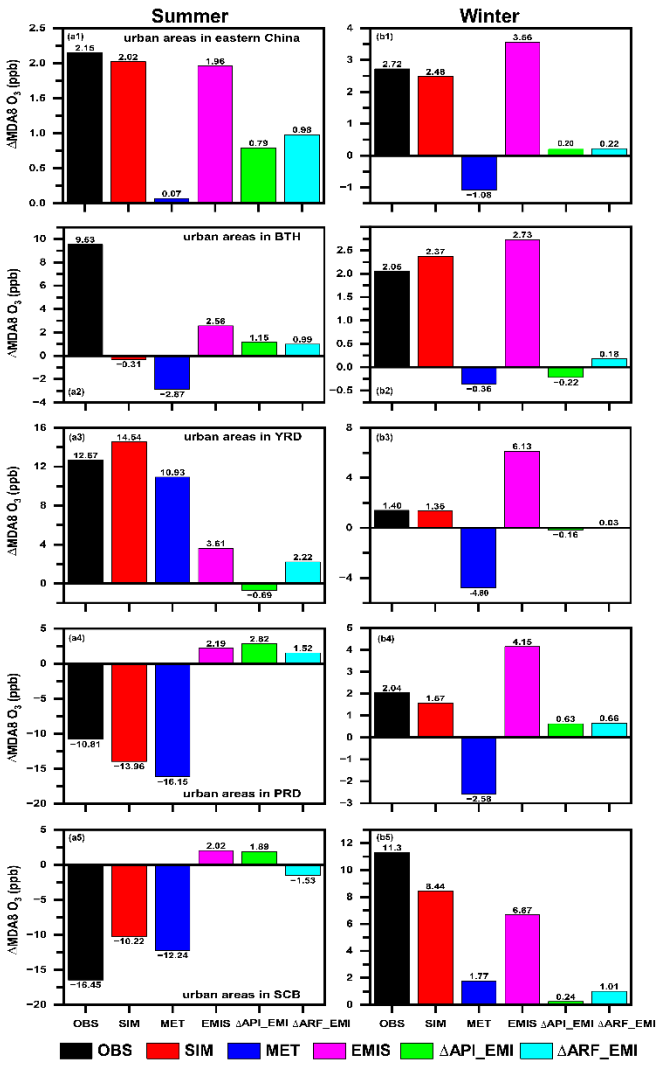

Figure R7. The observed (OBS, black bars) and simulated (SIM, red bars) changes in (left) summer and (right) winter surface-layer MDA8 O_3 from 2013 to 2017. Contributions of changed meteorological conditions alone (MET, blue bars), changed anthropogenic emissions alone (EMI, purple bars), changed aerosol-photolysis interaction alone (ΔAPI_EMI, green bars), and changed aerosol-radiation feedback alone (ΔARF_EMI, cyan bars) are also shown. Observations are calculated from the monitoring sites in the analyzed region, while the corresponding gridded simulations are averaged for SIM. **(a1-b1)**, **(a2-b2)**, **(a3-b3)**, **(a4-b4)** and **(a5-b5)** represent the urban areas in eastern China, Beijing-Tianjin-Hebei (BTH), Yangtze River Delta (YRD), Pearl River Delta (PRD), and Sichuan Basin (SCB), respectively.

19. *L429-431, you mentioned "multi-pollutants coordinated emissions control strategies", can you specify this and give more details? Liu and Wang, 2020 suggested that "to reduce O_3 levels in major urban and industrial areas, VOC emission controls should be added to the current NOx-SO_2-PM policy". Does your research have similar insights, or can you make other recommendations that could help policymakers?*

Response:

Thanks for reviewer's suggestion. Our suggestion is consistent with Liu and Wang (2020), we hope that the government should not focus on the control of $PM_{2.5}$ pollution (NOx-SO_2-PM policy),

but should pay attention to the synergistic control of multiple pollutants such as O_3 and $PM_{2.5}$.

Technical corrections:

1. *L211, "353 stations" - > "353 meteorological stations"*

   Response:

   Thanks for your suggestion. We have added the "meteorological" in the revised manuscript. (**Page 9, Line 235**)

2. *Figure S5, "from 2013to" - > "from 2013 to"*

   Response:

   Thanks for your suggestion. We have changed the expression in the revised manuscript. (**Page 11 in supporting information**)

3. *Figure 6, "on the right side of each panel" - > "on the upper right side of each panel"*

   Response:

   According to the reviewer's suggestion, we have changed the expression in the revised manuscript. (**Page 37, Line 859**)

4. *Data and code availability should be added.*

   Response:

   According to the reviewer's suggestion, we have added the "Data availability" section in the revised manuscript. (**Page 22, Line 593-600**)

Reference:

Gao, J., Li, Y., Xie, Z., Hu, B., Wang, L., Bao, F., and Fan, S.: The impact of the aerosol reduction on the worsening ozone pollution over the Beijing-Tianjin-Hebei region via influencing photolysis rates, Sci. Total Environ., 821, 153197, https://doi.org/10.1016/j.scitotenv.2022.153197, 2022.

Liu, Y. and Wang, T.: Worsening urban ozone pollution in China from 2013 to 2017 – Part 2: The effects of emission changes and implications for multi-pollutant control, Atmospheric Chem. Phys., 20, 6323–6337, https://doi.org/10.5194/acp-20-6323-2020, 2020.

Lou, S., Liao, H., and Zhu, B.: Impacts of aerosols on surface-layer ozone concentrations in China through heterogeneous reactions and changes in photolysis rates, Atmos. Environ., 85, 123–138, https://doi.org/10.1016/j.atmosenv.2013.12.004, 2014.

Reference:

Atkinson, R.: Atmospheric chemistry of VOCs and NOx, Atmos Environ., 34, 2063–2101, https://doi.org/10.1016/S1352-2310(99)00460-4, 2000.

Edson, C. T., Ivan, H.-P. and Alberto, M.: Use of combined observational- and model-derived photochemical indicators to assess the O_3-NO_x-VOC System sensitivity in urban areas, Atmosphere., 8, 22.

https://doi.org/10.3390/ atmos8020022, 2017.

Gipson, G. L.: Science algorithms of the EPA Models-3 community multiscale air quality (CMAQ) modeling system: Chapter 16, process analysis, edited by: Byun, D. W. and Ching, J. K. S., Reported No. EPA/600/R-99/030, U.S. Environmental Protection Agency, Office of Research and Development, Washington, D.C., 1999.

Hong, C., Zhang, Q., Zhang, Y., Davis, S. J., Zhang, X., Tong, D., Guan, D., Liu, Z., and He, K.: Weakening aerosol direct radiative effects mitigate climate penalty on Chinese air quality, Nat. Clim. Change, 10, 845–850, https://doi.org/10.1038/s41558-020-0840-y, 2020.

Lakey, P. S. J., George, I. J., Whalley, L. K., Baeza-Romero, M. T., and Heard, D. E.: Measurements of the HO_2 Uptake Coefficients onto Single Component Organic Aerosols, Environmental Science & Technology, 49, 4878-4885, 10.1021/acs.est.5b00948, 2015.

Li, K., Chen, L., Ying, F., White, S. J., Jang, C., Wu, X., Gao, X., Hong, S., Shen, J., Azzi, M. and Cen, K: Meteorological and chemical impacts on ozone formation: a case study in Hangzhou, China, Atmos. Res., 196, https://doi.org/10.1016/ j.atmosres.2017.06.003, 2017.

Li, K., Jacob, D. J., Liao, H., Shen, L., Zhang, Q., and Bates, K. H.: Anthropogenic drivers of 2013–2017 trends in summer surface ozone in China, P. Natl. Acad. Sci. USA, 116, 422–427, https://doi.org/10.1073/pnas.1812168116, 2019.

Liu, Y. and Wang, T.: Worsening urban ozone pollution in China from 2013 to 2017 – Part 1: The complex and varying roles of meteorology, Atmos. Chem. Phys., 20, 6305–6321, https://doi.org/10.5194/acp-20-6305-2020, 2020a.

Liu, Y. and Wang, T.: Worsening urban ozone pollution in China from 2013 to 2017 – Part 2: The effects of emission changes and implications for multi-pollutant control, Atmos. Chem. Phys., 20, 6323–6337, https://doi.org/10.5194/acp-20-6323-2020, 2020b.

Lo, J. C.-F., Yang, Z. L., and Pielke Sr, R. A.: Assessment of three dynamical climate downscaling methods using the Weather Research and Forecasting (WRF) model, J. Geophys. Res., 113, D09112, https://doi.org/10.1029/2007jd009216, 2008.

Qiu, Y., Liao, H., Zhang, R., and Hu, J.: Simulated impacts of direct radiative effects of scattering and absorbing aerosols on surface layer aerosol concentrations in China during a heavily polluted event in February 2014, J. Geophys. Res. Atmos., 122, 5955–5975, doi:10.1002/2016JD026309, 2017.

Seinfeld, J. H. and Pandis, S. N.: Atmospheric Chemistry and Physics: from Air Pollution to Climate Change, second ed., John Wiley and Sons, 2006.

Shao, M., Wang, W. J., Yuan, B., Parrish, D. D., Li, X., Lu, K. D., Wu, L. L., Wang, X. M., Mo, Z. W., Yang, S. X., Peng, Y. W., Kuang, Y., Chen, W. H., Hu, M., Zeng, L. M., Su, H., Cheng, Y. F., Zheng, J. Y., Zhang, Y. H.: Quantifying the role of $PM_{2.5}$ dropping in variations of ground-level ozone: Inter-comparison between Beijing and Los Angeles, Sci. Total Environ., https://doi.org/10.1016/j.scitotenv.2021.147712, 2021.

Shu, L., Wang, T., Han, H., Xie, M., Chen, P., Li, M., and Wu, H.: Summertime ozone pollution in the Yangtze River Delta of eastern China during 2013–2017: Synoptic impacts and source apportionment, Environ. Pollut., 257, 113631, https://doi.org/10.1016/j.envpol.2019.113631, 2020.

Shu, L., Xie, M., Wang, T., Gao, D., Chen, P., Han, Y., Li, S., Zhuang, B., and Li, M.: Integrated studies of a regional ozone pollution synthetically affected by subtropical high and typhoon system in the Yangtze River Delta region, China, Atmos. Chem. Phys., 16, 15801–15819, https://doi.org/10.5194/acp-16-15801- 2016, 2016.

Sillman, S.: The relation between ozone, NO_x and hydrocarbons in urban and polluted rural environments, Atmos. Environ., 33, 1821-1845, https://doi.org/ 10.1016/S1352-2310(98)00345-8, 1999.

Taketani, F., Kanaya, Y., and Akimoto, H.: Heterogeneous loss of HO2 by KCl, synthetic sea salt, and natural seawater aerosol particles, Atmospheric Environment, 43, 1660-1665, 2009.

Tan Z, Hofzumahaus A, Lu K, Brown SS, Holland F, Huey LG, et al. No Evidence for a Significant Impact of Heterogeneous Chemistry on Radical Concentrations in the North China Plain in Summer 2014. Environ. Sci. Technolc. 54, 5973-5979, 2020.

Wang, N., Lyu, X., Deng, X., Huang, X., Jiang, F., and Ding, A.: Aggravating O3 pollution due to NOx emission control in eastern China, Sci. Total Environ., 677, 732–744, 2019.

Yang, H., Chen, L., Liao, H., Zhu, J., Wang, W., and Li, X.: Impacts of aerosol–photolysis interaction and aerosol–radiation feedback on surface-layer ozone in North China during multi-pollutant air pollution episodes, Atmos. Chem. Phys., 22, 4101–4116, https://doi.org/10.5194/acp-22-4101-2022, 2022.

Zhang, B., Wang, Y., and Hao, J.: Simulating aerosol–radiation–cloud feedbacks on meteorology and air quality over eastern China under severe haze conditionsin winter, Atmos. Chem. Phys., 15, 2387–2404, https://doi.org/10.5194/acp-15-2387-2015, 2015.

Zhao, B., Wang, S., Donahue, N. M., Chuang, W., Ruiz, L. H., Ng, N. L., Wang, Y., and Hao, J.: Evaluation of One-Dimensional and Two-Dimensional Volatility Basis Sets in Simulating the Aging of Secondary Organic Aerosol with Smog-Chamber Experiments, Environ. Sci. Technol., 49, 2245–2254, doi:10.1021/es5048914, 2015.

Zhu, J., Chen, L., Liao, H., Yang, H., Yang, Y., and Yue, X.: Enhanced PM2.5 Decreases and O3 Increases in China During COVID-19 Lockdown by Aerosol-Radiation Feedback, Geophys. Res. Lett., 48, https://doi.org/10.1029/2020GL090260, 2021.

Zhou, M., Zhang, L., Chen, D., Gu, Y., Fu, T.-M., Gao, M., Zhao, Y., Lu, X. and Zhao, B.: The impact of aerosol-radiation interactions on the effectiveness of emission control measures, Environmental Research Letters, 14(2), 024002, https://doi.org/10.1088/1748-9326/aaf27d, 2019.

Zou Q, Song H, Tang M, Lu K. Measurements of HO_2 uptake coefficient on aqueous $(NH_4)_2SO_4$ aerosol using aerosol flow tube with LIF system. Chinese Chemical Letters 2019; 30: 2236-2240.

Thank you very much for your comments and suggestions.

Response to Comments of Reviewer #2

(comments in *italics*)

Manuscript number: EGUSPHERE-2023-2393

Title: Weakened aerosol-radiation interaction exacerbating ozone pollution in eastern China since China's clean air actions

This study examines the role of aerosol-radiation interaction (ARI), decomposed into aerosol-photolysis interaction (API) and aerosol-radiation feedback (ARF) on surface ozone concentration in China. Surface ozone increased remarkable in eastern China, contrasting the dramatic decline of $PM_{2.5}$ concentrations. It is therefore necessary to investigate the reasons for the ozone increase. The study found that reduced ARI due to decreased PM concentrations contributes to ozone production, with API playing a more important role than ARF. The regional differences are also briefly discussed. I think this is a nice study that is helpful in understanding the recent ozone increase in China. I only have a few minor comments.

Response:

Thanks to the reviewer for the valuable comments and suggestions which are very helpful for us to improve our manuscript. We have revised the manuscript carefully, as described in our point-to-point responses to the comments.

1. *A previous study seemed to indicate that chemical processes associated with $PM_{2.5}$ reduction, i.e., reduced removing rate of hydroperoxy radicals, is the main reason for the ozone increase in eastern China (Li et al., 2019, PNAS). I wonder how this effect compare to the ARI discussed in this study?*

Response:

As Li et al. (2019) did not directly quantify the extent of O_3 increase by weakened aerosol heterogeneous reactions, we use the results of Liu and Wang. (2020) for comparison. The increased MDA8 O_3 concentration over urban areas in summer caused by weakened aerosol-radiation interaction in this study is 1.77 ppb, which is compared to the value of 2.12 ppb increase caused by weakened aerosol heterogeneous reactions quantified by Liu and Wang (2020). According to the reviewer's comments, we have added this sentence in the revised manuscript. (**Page 18, Line 485-488**)

2. *In the WRF-Chem experiments, the authors zeroed off aerosol optical properties to exclude ARF. I wonder if aerosol microphysical properties are still included? This may affect cloud properties and still impact the radiation budget.*

Response:

The effects of aerosols on microphysical properties were not consider in this work. The most common approach to assessing the impact of aerosol-cloud interactions on air quality in model simulation is to assume a prescribed vertically uniform cloud droplet number concentration (Zhang et al., 2015; Zhao et al., 2017). In this study, we turned off aerosol optical properties in the optical

module which could not affect the cloud properties.

Figure R1 shows the spatial distributions of simulated summer and winter cloud droplet number concentration (CDNC) from BASE_17E17M and NOALL_17E17M cases in the daytime (08:00–17:00 LST). Analyzing Fig. R1, the CDNC distribution and concentration of BASE and NOALL has barely changed. Therefore, we zeroed off aerosol optical properties to exclude ARI with less impact on the cloud.

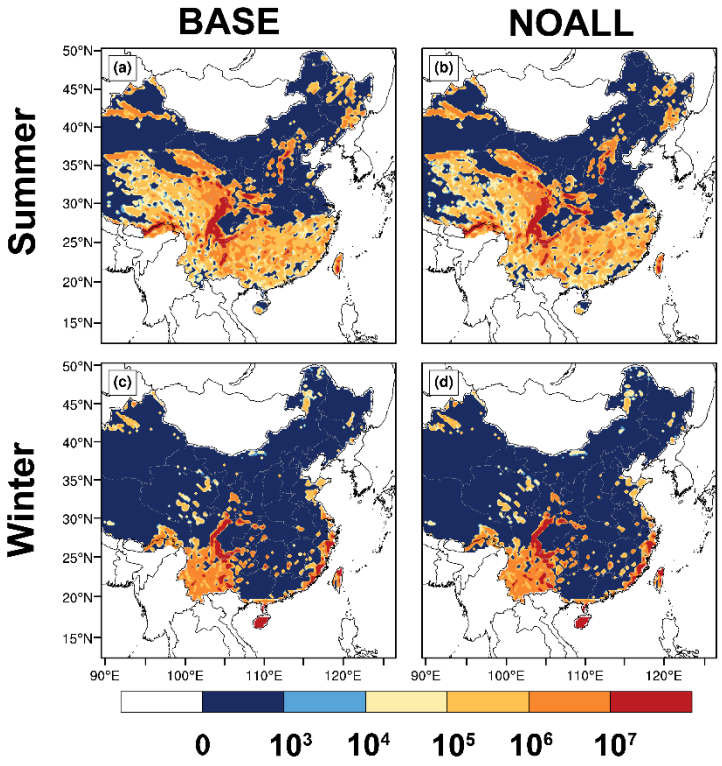

Figure R1. Spatial distributions of simulated summer (upper) and winter (bottom) cloud droplet number concentration (CDNC) from BASE_17E17M and NOALL_17E17M cases in the daytime (08:00–17:00 LST).

3. *Section 3.2, model evaluation: why not also evaluate VOCs, which is also an important precursor for ozone?*

Response:

Thanks for reviewer's suggestion. In this study, we did not evaluate VOCs due to the lack of measurements of VOCs over the China. However, the China's Ministry of Environmental Protection will include VOCs as a routine monitoring object in the future. Therefore, we will include this comparison in our future work.

4. *Line 87 and associated discussions: Does ARI always suppress O_3 formation? Could the change the meteorological variables through ARF increase O_3 concentration, say by reducing RH or increasing regional transport?*

Response:

Yang et al. (2022) reported that ARF reduced the planetary boundary layer height in North China, leading to an increase in VOCs and NO_x concentrations, which is favorable for ozone chemical production. Gao et al. (2018) also found that ARF can enhance ozone chemical

production through this pathway. Therefore, ARF can increase O_3 concentration by influencing the meteorological variables, e.g. by reducing the height of the planetary boundary layer.

5. *I suggest the authors discuss more about the summer-winter differences. Wintertime has much less radiation and lower temperature, so ARI is in general much lower. In summer, meteorology seems to make large contributions than emission changes (Figure 4, left column), what might be the reason?*

Response:

Focusing on the four developed city clusters, compared with 2013, the meteorological conditions in the summer of 2017 promoted the generation of O_3 in the YRD region (Fig. R2(a3)), but suppressed the generation of O_3 in the BTH (Fig. R2(a2)), PRD (Fig. R2(a4)) and SCB (Fig. R2(a5)) regions. In PRD and SCB, the changes in MDA8 O_3 due to meteorology even have a greater impact than that by emission changes, which highlights the significant role of meteorology on summer O_3 variations. **(Page 13, Line 343-349)**

According to the comments of Reviewer#1, another three widely used chemical mechanisms, i.e., RADM2 gas-phase chemistry coupled with MADE/SORGAM aerosol module (RADM2-MADE/SORGAM for short), CBMZ gas-phase chemistry coupled with MADE/SORGAM aerosol module (CBMZ-MADE/SORGAM for short), and MOZART gas-phase chemistry coupled with MOSAIC aerosol module (MOZART-MOSAIC for short), that include SOA formation are also applied to assess the impact of aerosol-radiation interaction (ARI) on O_3 during summer and winter is added in the discussion section. (**Page 18-19, Line 497-536**)

In summer, solar radiation flux reaches its maximum and atmospheric temperature are also higher than that in winter. The atmospheric warming can alter tropospheric O_3 concentrations by modulating the chemical kinetic, dynamic processes or biogenic emissions. Warmer temperatures often coincide with other meteorological conditions favorable to O_3 production, such as stagnation air and reduced cloud cover (Vukovich, 1995). This may be the reason why meteorological effect on O_3 is greater than that by emissions changes.

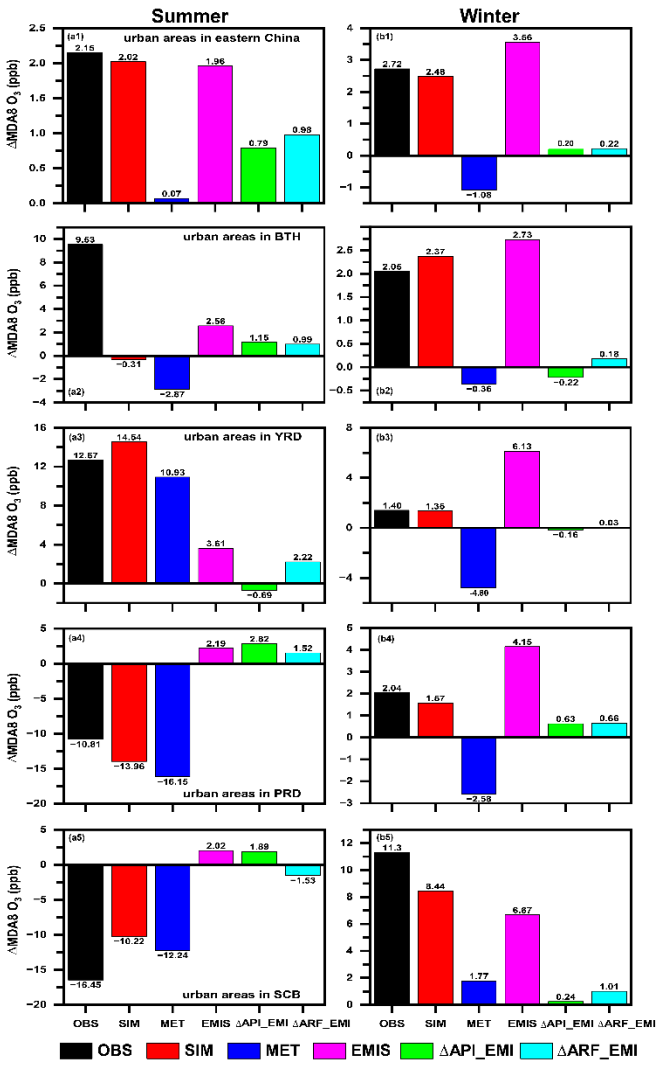

Figure R2. The observed (OBS, black bars) and simulated (SIM, red bars) changes in (left) summer and (right) winter surface-layer MDA8 O_3 from 2013 to 2017. Contributions of changed meteorological conditions alone (MET, blue bars), changed anthropogenic emissions alone (EMI, purple bars), changed aerosol-photolysis interaction alone (ΔAPI_EMI, green bars), and changed aerosol-radiation feedback alone (ΔARF_EMI, cyan bars) are also shown. Observations are calculated from the monitoring sites in the analyzed region, while the corresponding gridded simulations are averaged for SIM. **(a1-b1)**, **(a2-b2)**, **(a3-b3)**, **(a4-b4)** and **(a5-b5)** represent the urban areas in eastern China, Beijing-Tianjin-Hebei (BTH), Yangtze River Delta (YRD), Pearl River Delta (PRD), and Sichuan Basin (SCB), respectively.

6. *Figure 4: model seems to significantly underestimate the ozone change in BTH for summer (Figure 4a2). This area experienced the most ozone increases in the past decade. So it is important for the model to correctly represent ozone trend in this region. What might be the reason for this significant bias?*

Response:

Thanks for your suggestion. The reason for the underestimation over BTH in summer may be that this study did not consider the effect of changes in aerosol heterogeneous reactions, due to the uncertainty of the heterogeneous uptake value used in the numerical simulation. Li et al. (2019) found that the weakened uptake of HO_2 on aerosol surfaces was the main reason for the

O_3 increase over BTH. Therefore, the contributions of aerosol heterogeneous reactions to O_3 air quality will be discussed detailedly in our future work.

7. *Finally, the effects of API and ARF may not be independent, i.e., there may be nonlinear interaction between the two effects. This should be noted and discussed.*

Response:

Thanks for the reviewer's suggestion. A discussion of the separate treatment of API and ARF in this study has been added in the revised manuscript as follows: "There may be an interaction between API and ARF. However, in this study we discuss the role of API and ARF separately, which may ignore the effects of interactions between API and ARF on O_3. This may affect our results, and we will discuss their interaction in our future studies." (**Page 20, Line 557-560**)

Reference:

Gao, J. H., Zhu, B., Xiao, H., Kang, H. Q., Pan, C., Wang, D. D., and Wang, H. L.: Effects of black carbon and boundary layer interaction on surface ozone in Nanjing, China, Atmos. Chem. Phys., 18, 7081–7094, https://doi.org/10.5194/acp-18-7081-2018, 2018.

Li, K., Jacob, D. J., Liao, H., Shen, L., Zhang, Q., and Bates, K. H.: Anthropogenic drivers of 2013–2017 trends in summer surface ozone in China, P. Natl. Acad. Sci. USA, 116, 422–427, https://doi.org/10.1073/pnas.1812168116, 2019.

Liu, Y. and Wang, T.: Worsening urban ozone pollution in China from 2013 to 2017 – Part 2: The effects of emission changes and implications for multi-pollutant control, Atmos. Chem. Phys., 20, 6323–6337, https://doi.org/10.5194/acp-20-6323-2020, 2020.

Vukovich F. M.: Regional-scale boundary layer ozone variations in the eastern United States and their association with meteorological variations, Atmos. Environ., 29, 2259-2273, 1995.

Yang, H., Chen, L., Liao, H., Zhu, J., Wang, W., and Li, X.: Impacts of aerosol–photolysis interaction and aerosol–radiation feedback on surface-layer ozone in North China during multi-pollutant air pollution episodes, Atmos. Chem. Phys., 22, 4101–4116, https://doi.org/10.5194/acp-22-4101-2022, 2022.

Zhang, B., Wang, Y., and Hao, J.: Simulating aerosol–radiation–cloud feedbacks on meteorology and air quality over eastern China under severe haze conditionsin winter, Atmos. Chem. Phys., 15, 2387–2404, https://doi.org/10.5194/acp-15-2387-2015, 2015.

Zhao, B., Liou, K.-N., Gu, Y., Li, Q., Jiang, J. H., Su, H., He, C., Tseng, H.-L. R., Wang, S., Liu, R., Qi, L., Lee, W.-L., and Hao, J.: Enhanced $PM_{2.5}$ pollution in China due to aerosol-cloud interactions, Scient. Rep., 7, 4453, https://doi.org/10.1038/s41598-017-04096-8, 2017.

Thank you very much for your comments and suggestions.

Response to Comments of Reviewer #3

(comments in *italics*)

Manuscript number: EGUSPHERE-2023-2393

Title: Weakened aerosol-radiation interaction exacerbating ozone pollution in eastern China since China's clean air actions

The manuscript focuses on the aerosol-radiation interaction (ARI), discussing how this process has changed in the context of the abrupt aerosol decrease in East China during 2013-2017, and evaluates its contribution to the recent ozone increase in China. ARI is divided into aerosol-photolysis interaction (API) and aerosol-radiation feedback (ARF), with the WRF-Chem model used to quantify these impacts. The authors have found non-negligible ozone increase resulting from the aerosol decrease through the API and ARF processes, which has implications for the synergistic control of aerosol and ozone. This is an interesting topic and I believe it can make a novel contribution to the community. However, several important aspects need to be addressed before it can be published in ACP.

Response:

Thanks to the reviewer for the valuable comments and suggestions which are very helpful for us to improve our manuscript. We have revised the manuscript carefully, as described in our point-to-point responses to the comments.

General comments:

1. *The study focuses on aerosol-radiation interaction (ARI), which is split into two parts: the direct aerosol impact on radiation through scattering and absorbing (API) and the subsequent feedback on meteorology (ARF), with both influencing ozone concentrations. However, the Introduction Section could do a better job at breaking down these concepts. A detailed explanation of the distinctions between API and ARF would aid comprehension. Also, elucidating the specific ARF-related meteorological variables and their influences on ozone concentrations would be beneficial. Regarding the cited papers, such as Hong et al. (2020) and Zhu et al. (2021), the authors may consider including additional information about which ARF-related meteorological factors have been identified as important in affecting ozone concentrations.*

Response:

Thanks to the reviewer for the valuable comments and suggestions, we have added this information in the revised manuscript as follows: "API can affect O_3 directly by reducing the photochemical reactions, which weaken the chemical contribution and reduce the surface O_3 concentrations. ARF indirectly affects O_3 concentrations by altering meteorological variables, e.g. by reducing the height of the planetary boundary layer. The suppressed planetary boundary layer can weaken the vertical mixing of O_3 by turbulence and affect the concentration of O_3 precursors. Hong et al. (2020) used WRF-CMAQ in conjunction with future emission scenarios

to find that weakened ARF due to reduced aerosol concentration has either negative or positive impacts on the daily maximum 1-h average O_3 concentration in eastern China from 2010 to 2050 due to the changed precursor level caused by the weakened ARF. By using WRF-CMAQ, Liu and Wang (2020b) reported that weakened API could increase the MDA8 O_3 concentrations by 0.3 ppb in urban areas from 2013 to 2017. Zhu et al. (2021) used WRF-Chem to investigate the impact of weakened ARF on air pollutants over NCP during COVID-19 lockdown and reported that the weakened ARF would increase the O_3 concentrations by 7.8% due to the increased northwesterly and planetary boundary layer height caused by the weakened ARF." (**Page 4-5, Line 95-110**)

2. *In Section 3.2, could the authors talk more about how well the model is doing in reproducing the observed decrease in $PM_{2.5}$ levels from 2013-2017. This analysis is crucial for assessing whether the model's effectively capturing the weakening of ARI.*

Response:

Thanks for your suggestion. Figure R1 demonstrates the spatial distribution of changed summer (left) and winter (right) surface (a, b) $PM_{2.5}$ and (c, d) MDA8 O_3 from 2013 to 2017. As shown in Figs. R1(a) and R1(b), the observed concentrations of $PM_{2.5}$ in eastern China are significantly reduced both in summer (-16.2 μg m^{-3}) and winter (-56.0 μg m^{-3}), and these changes can be well captured by the model (-14.3 μg m^{-3} for summer and -49.8 μg m^{-3} for winter). Therefore, the model can reproduce the observed decrease in $PM_{2.5}$ levels from 2013 to 2017. As shown in Figs. R1(c) and R1(d), the model reasonably well reproduces the seasonal patterns of changed surface MDA8 O_3 over the eastern China during summer and winter from 2013 to 2017. In summer, both the observations and simulations show the increased (decreased) MDA8 O_3 in YRD (PRD and SCB), while the model can not simulate the positive changes in MDA8 O_3 over BTH, and the potential reasons may be that this study did not consider the effect of changes in aerosol heterogeneous reactions. Li et al. (2019) found that the weakened uptake of HO_2 on aerosol surfaces was the main reason for the O_3 increase over BTH. In contrast to the changes in summer, observed MDA8 O_3 in winter generally increased over the eastern China, which can be well reproduced by the model. (**Page 12, Line 308-324**)

According to the reviewer's comments, Figure R1 is added in the model evaluation section. (**Figure 3**)

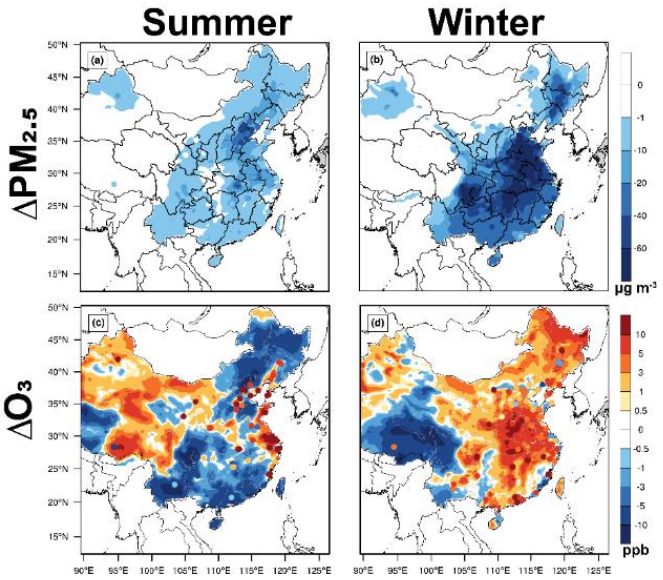

Figure R1. Spatial distribution of changed summer (left) and winter (right) surface (a, b) $PM_{2.5}$ and (c, d) MDA8 O_3 from 2013 to 2017.

3. *Section 4 needs to be better organized for clarity. I've outlined some areas for consideration:*

3.1. *The titles suggest Section 4.1 should focus on ΔO_3_MET and ΔO_3_EMI, while 4.2 should be devoted to ΔO_3_ΔARI_EMI. However, there is content overlap since 4.1 also examines ΔO_3_ΔARI_EMI, which obscures the distinctions between the two subsections.*

Response:

Thanks for your suggestion. We have changed this in revised manuscript. Section 4.1 focuses only on the ΔO_3_MET and ΔO_3_EMI, and the results of the ΔO_3_ΔARI_EMI in urban areas have been moved to Section 4.2. (**Page 12-13, Line 326-349**)

3.2. *Section 4.1 discusses ΔO_3_MET, ΔO_3_EMI, and ΔO_3_ΔARI_EMI at sparse polluted grids (so-called urban areas) while 4.2 talks about ΔO_3_ΔARI_EMI in term of regional averages. It is unclear why the discussion about ΔO_3_MET and ΔO_3_EMI focuses only on urban polluted regions. Also, the rationale for addressing urban ΔO_3_ΔARI_EMI prior to regional averages is not evident, particularly when urban results mirror the regional ones, though more pronounced. I recommend relocating the OBS-SIM ozone change comparison from Section 4.1 to Section 3.2 (to combine it with $PM_{2.5}$ change evaluation) and discussing regional ΔO_3_ΔARI_EMI before the urban analysis.*

Response:

Thanks for your suggestion. The comparison of O_3 change from 2013 to 2017 has been combined with the comparison of $PM_{2.5}$ change in Section 3. The detailed information can be found in the answer to your second question.

According to review's suggestion, in the revised manuscript we first discussed the effects of weakened ARI on O_3 at the regional level, and then in urban areas. **(Page 14-18, Line 383-495)**

3.3. *Section 4.3 and Figure 7 are quite similar to Section 4.2 and Figure 5. Please consider merging Sections 4.2 and 4.3.*

Response:

Thanks for your suggestion. We've combined these two sections in the revised manuscript.

4. *Could the authors explain why ΔO_3_ΔARI_EMI displays a much steeper spatial gradient in summer compared to winter (Fig. 5), whereas the $PM_{2.5}$ change suggest the opposite pattern (Fig. S8)? How does meteorology contribute to this discrepancy? Moreover, why does summertime ΔO_3_ΔARI_EMI exhibit both positive (e.g., NCP) and negative (e.g., Shandong province) values, even though the $PM_{2.5}$ decreases universally?*

Response:

The reason may be that the solar radiation flux reaches its maximum in summer seasons. The changes in meteorological variables are larger in summer than in winter due to the weakened ARI, despite the substantial decrease in aerosol concentrations during winter. Meteorology is likely to be a major contributor to this discrepancy.

Although the concentration of $PM_{2.5}$ is reduced uniformly, the changes in the components of $PM_{2.5}$ are different in different locations, resulting in different changes in single scattering albedo (SSA). As shown in Fig. R2, SSA did not change in NCP, but became smaller in Shandong Province, which may be the reason for the different changes in O_3 in these two regions. Furthermore, Fig. S7(b3) and S7(c3) show that weakened aerosol-radiation interaction leads to a decrease in T_2 but an increase in RH_2 over Shandong, which is also unfavourable for O_3 production. This could also be one of the reasons why weakened aerosol-radiation interaction leads to O_3 reduction in Shandong Province.

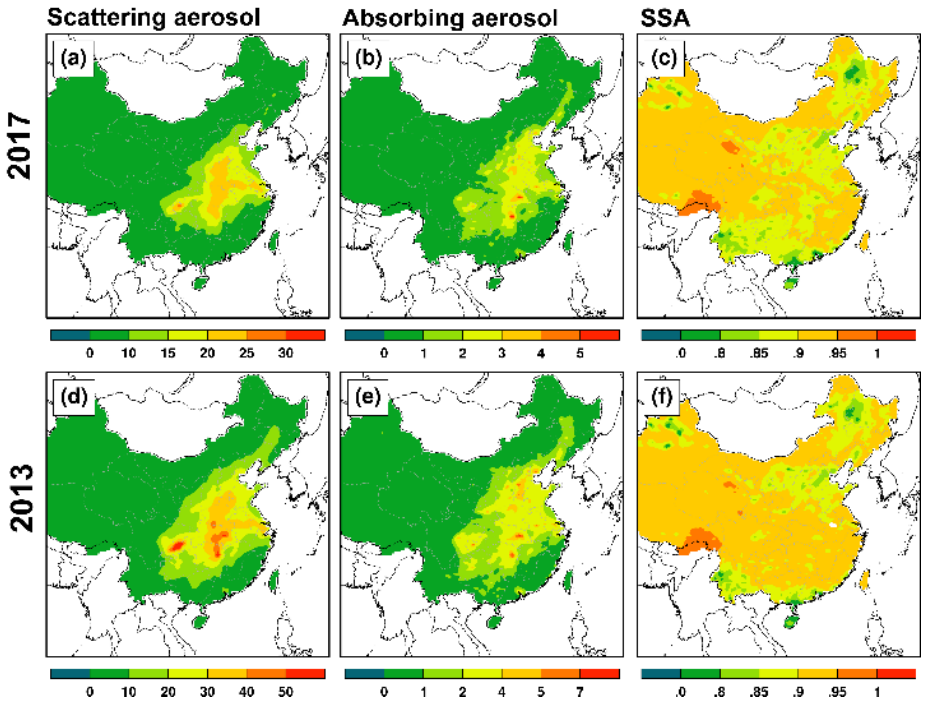

Figure R2. Spatial distribution of **(a, d)** scattering aerosol, **(b, e)** absorbing aerosol, and **(c, f)** single scattering albedo (SSA) of BASE_17E17M (upper) and BASE_13E17M (bottom) cases.

5. *From my understanding, the reduced impact of ARI on ozone is a component of the anthropogenic impact on ozone, since the reduction in ARI results from changes in anthropogenic emissions. However, the phrasing in Lines 396-398 and abstract (specifically the use of "superimposed") suggest that ΔO_3_ΔARI_EMI is and additional, separate effect rather than being nested within the broader anthropogenic impact on ozone. Please clarify.*

Response:

Thanks for your suggestion. Figure R3 shows the changed summer and winter surface-layer MDA8 O_3 concentrations caused by anthropogenic emission reduction from 2013 to 2017 with (ΔO_3_EMI) and without (ΔO_3_NOARI) ARI, including the effects of weakened ARI on the effectiveness of emission reduction for O_3 air quality (ΔO_3_ΔARI_EMI, which is also equal to ΔO_3_EMI minus ΔO_3_NOARI). As shown in Figs. R3(a1) and R3(a4), the surface-layer MDA8 O_3 concentrations increased in urban areas during summer and increased uniformly in winter due to anthropogenic emission reduction from 2013 to 2017 without the impact of ARI. The plots in the second column (Figs. R3(a2) and R3(a5)) are the same as R3(a1) and R3(a4) except that the impact of ARI is applied. When the effect of ARI is considered, the concentrations of MDA8 O_3 are increased more than that when ARI is not considered. The differences between plots in second column and first column are the consequences of weakened ARI resulted from anthropogenic emission reduction on MDA8 O_3 concentrations. As shown in Figs. R3(a3) and R3(a6), the concentrations of MDA8 O_3 are increased in both summer and winter over eastern China. Therefore, ΔO_3_ΔARI_EMI makes the superimposed impact on the effectiveness of anthropogenic emission reduction for the increased MDA8 O_3 concentrations from 2013 to 2017 over eastern China.

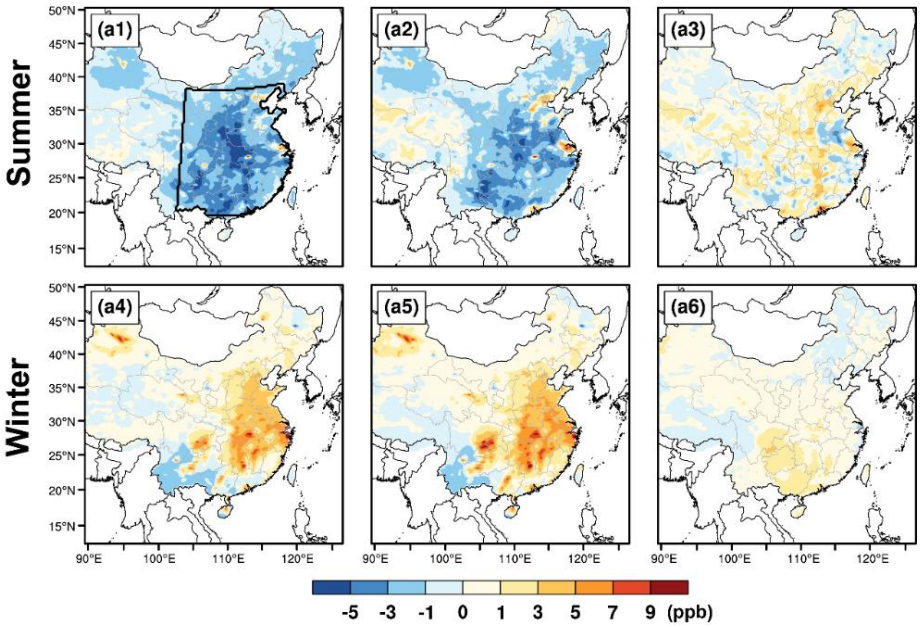

Figure R3. Spatial distribution of changed summer (upper) and winter (bottom) surface-layer MDA8 O_3 concentrations from sensitivity simulations. **(a1, a4)** Effects of anthropogenic emission reduction on MDA8 O_3 without ARI. **(a2, a5)** Effects of anthropogenic emission reduction on MDA8 O_3 with ARI. **(a3, a6)** Effects of weakened ARI on the effectiveness of emission reduction for O_3 air quality.

6. *In the Abstract, needs to explicitly clarify that the numbers presented are derived*

from different analysis. Lines 28-29 are for sparse polluted grids, while Lines 33-35 are for regional averages. Otherwise, readers may erroneously interpret the ratio between the numbers in Lines 33-35 and Lines 28-29 as the contribution of ARI to the total anthropogenic impacts.

Response:

Thanks for your suggestion. We've added this information in the revised manuscript as follows:

"Sensitivity experiments show that the decreased anthropogenic emissions play a more prominent role for the increased MDA8 O_3 both in summer (+1.96 ppb vs. +0.07 ppb) and winter (+3.56 ppb vs. -1.08 ppb) than the impacts of changed meteorological conditions in urban areas. (**Page 2, Line 27-31**)

The weakened ARI due to decreased anthropogenic emission aggravates the summer (winter) O_3 pollution by +0.81 ppb (+0.63 ppb) averaged over eastern China, with weakened API and ARF contributing 55.6% (61.9%) and 44.4% (38.1%), respectively. This superimposed effect is more significant for urban areas during summer (+1.77 ppb). (**Page 2, Line 33-37**)"

Specific comments:

1. Line 61, natural emissions are also an important precursor source. Please clarify.

   Response:

   According to the reviewer's suggestion, we have changed the expression in the revised manuscript. (**Page 3, Line 65-67**)

2. Section 3.2, it should be "Fig. 2" instead of "Figs. 2". Similar typos are found in other places, e.g., Line 290, 302, 348. Please check.

   Response:

   Thanks for your suggestion. Since it's followed by a plural, we use "Figs".

3. Line 293, delete "will".

   Response:

   Deleted.

4. Lines 310-312 and figure 4, please clarify in the figure caption that ARI_EMI can be obtained by summing the bars of API_EMI and ARF_EMI.

   Response:

   Thanks for your suggestion. We have defined the ΔO_3_ΔARI_EMI = ΔO_3_ΔARF_EMI + ΔO_3_ΔAPI_EMI in the revised manuscript. (**Page 15, Line 405-406**)

5. Lines 353-354 and figure 5, the numbers mentioned in the text are inconsistent with those presented in the figure. Please correct.

   Response:

   Correct.

6. Figure 6, the first x-axis label should be "ARI" instead of "ALL".

   Response:

   Thanks for your suggestion. We have changed the expression in the revised manuscript. (**Page 37**)

Reference:

Hong, C., Zhang, Q., Zhang, Y., Davis, S. J., Zhang, X., Tong, D., Guan, D., Liu, Z., and He, K.: Weakening aerosol direct radiative effects mitigate climate penalty on Chinese air quality, Nat. Clim. Change, 10, 845–850, https://doi.org/10.1038/s41558-020-0840-y, 2020.

Li, K., Jacob, D. J., Liao, H., Shen, L., Zhang, Q., and Bates, K. H.: Anthropogenic Drivers of 2013–2017 Trends in Summer Surface Ozone in China, P. Natl. Acad. Sci. USA, 116, 422–427, https://doi.org/10.1073/pnas.1812168116, 2019.

Liu, Y. and Wang, T.: Worsening urban ozone pollution in China from 2013 to 2017 – Part 2: The effects of emission changes and implications for multi-pollutant control, Atmos. Chem. Phys., 20, 6323–6337, https://doi.org/10.5194/acp-20-6323-2020, 2020b.

Zhu, J., Chen, L., Liao, H., Yang, H., Yang, Y., and Yue, X.: Enhanced PM2.5 Decreases and O3 Increases in China During COVID-19 Lockdown by Aerosol-Radiation Feedback, Geophys. Res. Lett., 48, https://doi.org/10.1029/2020GL090260, 2021.

Thank you very much for your comments and suggestions.

Weakened aerosol-radiation interaction exacerbating ozone pollution in eastern China since China's clean air actions

Hao Yang[1,2], Lei Chen[1], Hong Liao[1], Jia Zhu[1], Wenjie Wang[3], Xin Li[3]

[1]Jiangsu Key Laboratory of Atmospheric Environment Monitoring and Pollution Control, Jiangsu Collaborative Innovation Center of Atmospheric Environment and Equipment Technology, School of Environmental Science and Engineering, Nanjing University of Information Science & Technology, Nanjing 210044, China

[2]College of Materials Science and Engineering, Guizhou Minzu University, Guiyang 550025, China

[3]State Joint Key Laboratory of Environmental Simulation and Pollution Control, College of Environmental Sciences and Engineering, Peking University, Beijing 100871, China

Correspondence to: Lei Chen (chenlei@nuist.edu.cn) and Hong Liao (hongliao@nuist.edu.cn)

Abstract

Since China's clean air action, $PM_{2.5}$ air quality has been improved while ozone (O_3) pollution has been becoming severe. Here we apply a coupled meteorology-chemistry model (WRF-Chem) to quantify the responses of aerosol-radiation interaction (ARI), including aerosol-photolysis interaction (API) related to photolysis rate change and aerosol-radiation feedback (ARF) related to meteorological fields change, to anthropogenic emission reductions from 2013 to 2017, and their contributions to O_3 increases over eastern China in summer and winter. Sensitivity experiments show that the decreased anthropogenic emissions play a more prominent role for the increased MDA8 O_3 both in summer (+1.96 ppb vs. +0.07 ppb) and winter (+3.56 ppb vs. -1.08 ppb) than the impacts of changed meteorological conditions in urban areas. The decreased $PM_{2.5}$ caused by emission reduction can result in a weaker impact of ARI on O_3 concentrations, which poses a superimposed effect on the worsened O_3 air quality. The weakened ARI due to decreased anthropogenic emission aggravates the summer (winter) O_3 pollution by +0.81 ppb (+0.63 ppb) averaged over eastern China, with weakened API and ARF contributing 55.6% (61.9%) and 44.4% (38.1%), respectively~~; t~~. This superimposed effect is more significant for urban areas during summer (+1.77 ppb). Process analysis indicates that the enhanced chemical production is the dominant process for the increased O_3 concentrations caused by weakened ARI both in summer and winter. This study innovatively reveals the adverse effect of weakened aerosol-radiation interaction due to decreased anthropogenic emissions on O_3 air quality, indicating~~;~~ more stringent coordinated air pollution control strategies should be made~~are needed~~ for significant improvements in future air quality ~~improvement~~.

1. Introduction

With the implementation of clean air action since 2013, $PM_{2.5}$ (particulate matter with an aerodynamic equivalent diameter of 2.5 micrometers or less) concentrations have decreased significantly in China (Zhai et al., 2019; Zhang et al., 2019). However, ozone (O_3) pollution is becoming worse and poses a significant challenge over eastern China, especially in the developed city clusters including Beijing-Tianjin-Hebei (BTH), Yangtze River Delta (YRD), Pearl River Delta (PRD), and Sichuan Basin (SCB) (Lu et al., 2018; Dang and Liao, 2019; Li et al., 2019; Li et al., 2021). According to observation data, Li et al. (2020) found that the daily maximum 8-h average O_3 concentrations (MDA8 O_3) increased at a rate of 1.9 ppb a^{-1} from 2013 to 2019 over eastern China. Elevated O_3 concentrations can not only decrease crop yield but also damage human health (Lelieveld et al., 2015; Yue et al., 2017; Mills et al., 2018). Therefore, it is essential to gain a comprehensive understanding about factors driving the increasing trend of O_3 in China in order to formulate effective prevention strategies.

As a secondary air pollutant, troposphere O_3 can be produced by nitrogen oxides (NO_x = NO + NO_2), carbon monoxide (CO), methane (CH_4) and volatile organic compounds (VOCs) in the presence of solar radiation through photochemical reactions (Atkinson, 2000; Seinfeld and Pandis, 2006). ~~Consequently, t~~The concentration of O_3 in the troposphere is influenced by changes in meteorological conditions (e.g., high temperature and low relative humidity) and its precursors emissions (e.g., NOx and VOCs) (Wang et al., 2019; Liu and Wang, 2020a,b; Shu et al., 2020). Most precursors are from anthropogenic sources, and some precursors can come from natural sources, such as biogenic VOCs and soil and lightning NOx.~~is closely related to changes in meteorological conditions and anthropogenic emissions (Wang et al., 2019; Liu and Wang, 2020a,b; Shu et al., 2020).~~ Moreover, particulates can also affect O_3 concentrations through aerosol-radiation interaction (ARI), including aerosol-photolysis interaction (API) and aerosol-radiation feedback (ARF) (Liao et al., 1999; Wang et al., 2016; Zhu et al., 2021; Yang et al., 2022), and heterogeneous chemistry on aerosol surface (Lou et al., 2014; Li et al., 2019; Liu and Wang, 2020b). Many

studies have found that the decreased $PM_{2.5}$ can be one of the driving factors contributing to the increased O_3 concentrations (Li et al., 2019; Liu and Wang, 2020b; Shao et al., 2021). Li et al. (2019) analyzed GEOS-Chem simulation results and pointed out that the reductions in $PM_{2.5}$ concentrations from 2013 to 2017 in North China Plain (NCP) could decrease the sink of HO_2 on aerosol surface, which would result in the increase in O_3 concentrations. When heterogeneous reactions were considered in WRF-CMAQ, Liu and Wang (2020b) found that decreased $PM_{2.5}$ concentrations weakened the uptake of reactive gases (mainly HO_2 and O_3) which led to the increase in O_3 concentrations over China from 2013 to 2017. However, the contribution of weakened aerosol-radiation interaction due to substantial decreases in $PM_{2.5}$ under clean air action to the increased O_3 has not been systematically quantified. Furthermore, previous studies mainly focus on the increased summer O_3 (Li et al., 2019; Liu and Wang, 2020a,b; Shu et al., 2020; Shao et al., 2021), but underlying reasons driven the changes in winter O_3 is unclear. Li et al. (2021) pointed out that O_3 pollution has been extended into cold seasons under the emission control measures. Therefore, this study aims to quantify the response of aerosol-radiation interaction to anthropogenic emission reduction from 2013 to 2017, with the mainly focus on the contribution to changed O_3 concentrations over eastern China both in summer and winter.

Aerosol-radiation interaction (ARI) can alter photolysis rates through aerosol-photolysis interaction (API) and meteorological variables through aerosol-radiation feedback (ARF) to influence the formation of~~suppress~~ O_3 ~~formation~~ (Yang et al., 2022). API can affect O_3 directly by reducing the photochemical reactions, which weaken the chemical contribution and reduce the surface O_3 concentrations. ARF indirectly affects O_3 concentrations by altering meteorological variables, e.g. by reducing the height of the planetary boundary layer. The suppressed planetary boundary layer can weaken the vertical mixing of O_3 by turbulence and affect the concentration of O_3 precursors. Hong et al. (2020) used WRF-CMAQ in conjunction with future emission scenarios to find that weakened ARF due to reduced aerosol concentration has either negative or positive impacts on the daily maximum 1-h average O_3 concentration in eastern China from 2010 to 2050 due to the changed precursor level caused by the weakened ARF~~led to an~~

~~increase in the daily maximum 1-h average O_3 concentration in eastern China from 2010 to 2050~~. By using WRF-CMAQ, Liu and Wang (2020b) reported that weakened API could increase the MDA8 O_3 concentrations by 0.3 ppb in urban areas from 2013 to 2017. Zhu et al. (2021) used WRF-Chem to investigate the impact of weakened ARF on air pollutants over NCP during COVID-19 lockdown and reported that the weakened ARF would increase the O_3 concentrations by 7.8% due to the increased northwesterly and planetary boundary layer height caused by the weakened ARF. In general, previous studies mainly examined the impact of either weakened ARF or API, systematic analysis about the total and the respective impacts of changed API and/or ARF on O_3 over eastern China both in summer and winter from 2013 to 2017 have not been conducted.

The objective of this manuscript is to examine the impacts of aerosol-radiation interactions (ARI), including the effects of aerosol-photolysis interaction (API) and aerosol-radiation feedback (ARF), on O_3 concentrations over eastern China both in summer and winter by using the online coupled WRF-Chem model, with the main focus on their responses to clean air action. Process analysis is also applied to explore the prominent physical/chemical process responsible for the changed impacts of API and/or ARF on surface O_3. This study is believed to provide insights into the role of weakened ARI on O_3 levels over eastern China not only in summer, but also in winter. In Section 2, we describe the model configuration, numerical experiments, observational data, and the integrated process rate analysis. Model evaluation is presented in Section 3. Results and discussions are presented ~~The presentation of model results and the corresponding analyses are exhibited~~ in Section 4. Conclusions are provided in Section 5.

2. Methodology

2.1 Model configuration

The model used in this study is an online-coupled meteorology-chemistry model, Weather Research and Forecasting with Chemistry model (WRF-Chem v3.7.1), that can simulate meteorological fields and concentrations of gases and aerosols simultaneously (Grell et al., 2005; Skamarock et al., 2008). Figure S1 shows the

simulated domain that covers most regions of China with a horizontal resolution of 27 km and grid points of 167 (west–east) × 167 (south–north). The model contains 32 vertical levels extending from the surface to 50 hPa, with the first 16 layers located below 2 km to resolve fine boundary layer processes. The enclosed black line in Figure S1 represents the eastern China (22-41.5 °N, 102-123 °E), and the four heavily polluted regions are also selected for analysis, including BTH (36.0-41.5 °N, 113-119.5 °E), YRD (29.5-32.5 °N, 118-122 °E), PRD (21-23.5 °N, 112-116 °E), and SCB (27.5-31.5 °N, 102.5-107.5 °E), respectively.

The National Center for Environmental Prediction (NCEP) Final Analysis dataset (FNL) with a spatial resolution of 1° × 1° and 6-hour temporal resolution are used to provide the meteorological initial and lateral boundary conditions. The chemical initial and boundary conditions for the WRF-Chem model are taken from the outputs of Community Atmosphere Model with Chemistry (CAM-Chem).

The Carbon Bond Mechanism Z (CBM-Z) is applied as the gas-phase chemical mechanism (Zaveri and Peters, 1999), and the full 8-bin MOSAIC (Model for Simulating Aerosol Interactions and Chemistry) aerosol module with aqueous chemistry is used to simulate aerosol evolution (Zaveri et al., 2008). In MOSAIC module, aerosols are assumed to be internally mixed into 8 bins (0.039–0.078 μm, 0.078–0.156 μm, 0.156–0.312 μm, 0.312–0.625 μm, 0.625–1.25 μm, 1.25–2.5 μm, 2.5–5.0 μm and 5.0–10 μm), and each bin considers all major aerosol species, such as sulfate (SO_4^{2-}), nitrate (NO_3^-), ammonium (NH_4^+), black carbon (BC), organic carbon (OC), and other inorganic mass. The impacts of aerosols on photolysis rates are calculated by using the Fast-J scheme (Wild et al., 2000). The following physical parameterizations are used in WRF-Chem. The Rapid Radiative Transfer Model for general circulation models (RRTMG) scheme is used to treat both shortwave and longwave radiation in the atmosphere (Iacono et al., 2008). The Purdue Lin microphysics scheme (Lin et al., 1983) and the Grell 3D ensemble scheme (Grell, 1993) are used to describe the cloud microphysical and cumulus convective processes. The Noah land surface scheme (Chen and Dudhia, 2001) and the Monin-Obukhov surface scheme (Foken, 2006) are used to simulate land-atmosphere interactions. The planetary boundary layer is characterized

by Yonsei University PBL scheme (Hong et al 2006). The main physical and chemical schemes used in this study are summarised in Table S1.

In this study, Multi-resolution Emission Inventory for China (MEIC; http://www.meicmodel.org/) in 2013 and 2017 are used as the anthropogenic emissions of particles and gases (Zheng et al., 2018). Biogenic emissions are calculated online by using the Model of Emissions of Gases and Aerosols from Nature (MEGAN) developed by Guenther et al. (2006).

2.2 Numerical experiments

Seven sensitivity experiments are designed (Table 1). Here are the detailed descriptions:

(1) BASE_17E17M: This baseline experiment is coupled with the interactions between aerosol and radiation, which includes the impacts of API and ARF. Both the meteorological field and anthropogenic emission are from the year of 2017~~fixed at year 2017~~.

(2) BASE_13E13M: Same as BASE_17E17M, but the meteorological field and anthropogenic emission are from the year of 2013~~fixed at year 2013~~.

(3) NOAPI_17E17M: Same as BASE_17E17M, but the impact of API is not considered by turning off the aerosol effect in the photolysis module, following the method described in Yang et al. (2022).

(4) NOALL_17E17M: Same as BASE_17E17M, but neither the impact of API nor ARF is considered by zeroing the aerosol optical properties in the optical module, following the method described in Yang et al. (2022).

(5) BASE_13E17M: Same as BASE_17E17M, but the anthropogenic emission is ~~fixed~~ from the year of ~~at year~~ 2013.

(6) NOAPI_13E17M: Same as NOAPI_17E17M, but the anthropogenic emission is from the year of~~fixed at year~~ 2013.

(7) NOALL_13E17M: Same as NOALL_17E17M, but the anthropogenic emission is from the year of ~~fixed at year~~ 2013.

Figure 1 detailedly presents the schematic overview of designed numerical

experiments. As shown in Fig. 1, the differences between BASE_17E17M and BASE_13E13M (BASE_17E17M minus BASE_13E13M) represent the changed O_3 (ΔO_3) due to variations in meteorology and anthropogenic emissions from 2013 to 2017. The differences between BASE_13E17M and BASE_13E13M (BASE_13E17M minus BASE_13E13M) show the impact of changed meteorological conditions on O_3 (ΔO_3_MET) from 2013 to 2017. The differences between BASE_17E17M and BASE_13E17M (BASE_17E17M minus BASE_13E17M) indicate the impact of anthropogenic emission reductions on O_3 (ΔO_3_EMI) from 2013 to 2017.

The impacts of aerosol-radiation interaction (ARI) on O_3 under different anthropogenic emission scenarios (i.e., strong anthropogenic emission levels in year 2013, and weaker anthropogenic emission levels in year 2017) can be analyzed as the differences between BASE_17E17M and NOALL_17E17M (BASE_17E17M minus NOALL_17E17M, denote as ΔO_3_ARI_{17E}), and BASE_13E17M and NOALL_13E17M (BASE_13E17M minus NOALL_13E17M, denote as ΔO_3_ARI_{13E}). The ΔO_3_ARI_{17E} means that the impact of ARI on O_3 at the condition of both the meteorological field and anthropogenic emission are applied in the year 2017, and the ΔO_3_ARI_{13E} means that the effect of ARI on O_3 at the state of meteorological field used in the year 2017 and anthropogenic emission applied in the year 2013. In order to quantify the impacts caused by the decreased anthropogenic emission from 2013 to 2017, the impacts of changed meteorological variables should be removed by fixing the meteorological fields in year 2017 in sensitivity experiments. Thus, the impact of weakened ARI due to decreased anthropogenic emission from 2013 to 2017~~clean air action~~ on O_3 (denote as ΔO_3_ΔARI_EMI) can be quantified from the differences between ΔO_3_ARI_{17E} and ΔO_3_ARI_{13E}. Similarly, the impacts of weakened API (denote as ΔO_3_ΔAPI_EMI) and ARF (denote as ΔO_3_ΔARF_EMI) due to decreased anthropogenic emission on O_3 can also be estimated from the differences between (BASE_17E17M minus NOAPI_17E17M, denote as ΔO_3_API_{17E}) and (BASE_13E17M minus NOAPI_13E17M, denote as ΔO_3_API_{13E}), and between (NOAPI_17E17M minus NOALL_17E17M, denote as ΔO_3_ARF_{17E}) and (NOAPI_13E17M minus NOALL_13E17M, denote as ΔO_3_ARF_{13E}), respectively.

Detailed descriptions can be found in Fig. 1.

Simulation periods are integrated from 30 May to 30 June (denoted as summer) and 29 November to 31 December (denoted as winter) both in 2013 and 2017. To avoid potential deviations caused by long-term model integration, each simulation is re-initialized every eight days, with the first 40 hours as the model spin-up. The complete simulation includes five model cycles. Simulation results from the BASE_17E17M case during summer and winter are used to evaluate the model performance. If not otherwise specified, the time in this paper is the local time, and the synergetic impacts of ARF and API are equal to the impact of ARI (i.e., ARI=ARF+API).

2.3 Observational data

Meteorological observations of temperature (T_2), relative humidity (RH_2), wind speed (WS_{10}) and wind direction (WD_{10}) provided by the NOAA's National Climatic Data Center (https://www.ncei.noaa.gov/) are used to validate the model meteorological performance. In this study, 353 meteorological stations are selected and the locations are shown as red dots in Fig. S1. Observed surface $PM_{2.5}$, O_3 and NO_2 concentrations in eastern China are obtained from the China National Environmental Monitoring Center, which can be downloaded from http://beijingair.sinaapp.com. To ensure the data quality, a single site with at least 500 actual observations during the simulated period are used for model evaluation. A total of 1296 sites, as shown in Fig. 2a, are obtained. Photolysis rates of nitrogen dioxide (NO_2) ($J[NO_2]$) measured at the Peking University site (39.99 °N, 116.31 °E) are also used to evaluate the model performance.

2.4 Integrated process rate analysis

Process analysis techniques, i.e., integrated process rate (IPR) analysis, can be used in grid-based Eulerian models (e.g., WRF-Chem) to obtain contributions of each physical/chemical process to variations in pollutant concentrations. Eulerian models utilize the numerical technique of operator splitting to solve continuity equations for each species into several simple ordinary differential equations or partial differential equations that only contain the influence of one or two processes (Gipson, 1999).

In order to quantitatively elucidate individual contributions of physical and chemical processes to O_3 concentration changes due to weakened ARI, the integrated process rate (IPR) methodology is applied in this study. IPR analysis is an advanced tool to evaluate the key process for O_3 concentration variation (Shu et al., 2016; Zhu et al., 2021; Yang et al., 2022). In this study, the IPR analysis tracks hourly (e.g., one time step) contribution to O_3 concentration variation from four main processes, including vertical mixing (VMIX), net chemical production (CHEM), horizontal advection (ADVH), and vertical advection (ADVZ). VMIX is initiated by turbulent process and closely related to PBL development, which influences O_3 vertical gradients. CHEM represents the net O_3 chemical production (chemical production minus chemical consumption). ADVH and ADVZ represent transport by winds. We define ADV as the sum of ADVH and ADVZ.

3. Model Evaluation

Simulation results of BASE_17E17M are used to compare with the observations to evaluate the model performs before interpreting the impacts of aerosol-radiation interaction on surface-layer ozone concentration.

3.1 Evaluation for meteorology

Figure S2 shows the time series of observed and simulated T_2, RH_2, WS_{10}, and WD_{10} averaged over the 353 meteorological stations in China during summer and winter in 2017. Statistical performances of simulated meteorological parameters compared with ground-based observations are shown in Table 2. Simulations track well with observed T_2 with the correlation coefficient (R) of 0.99 and 0.92, but underestimate T_2 with the mean bias (MB) of -1.0 and -2.0 K in summer and winter, respectively. Simulated RH_2 agree reasonably well with observations with R of 0.97 and 0.87, and small normalized mean biases (NMB) are found in summer and winter with values of 3.2% and 3.5%, respectively. WS_{10} is slightly overpredicted with the MB of 1.6-2.1 m s^{-1}. The R and root-mean-square error (RMSE) of WS_{10} are 0.77-0.82 and 1.6-2.1 m s^{-1}, respectively. Large bias in wind speed can be partly caused by unresolved

topographical features (Jimenez and Dudhia, 2012). The NMB of WD_{10} ranges from -3.9% to -2.6% and the R ranges from 0.40 to 0.69, respectively. As shown in Fig. S3, the predicted J[NO_2] match well with the observations with R of 0.93-0.94 and NMB of 4.8%-12.3%. In general, the simulated meteorological variables fairly well agreement with the observations.

3.2 Evaluation for air pollutants

Figure 2 shows the spatial-temporal variations of observed and simulated near-surface $PM_{2.5}$, O_3 and NO_2 concentrations averaged over eastern China during summer and winter in 2017. As demonstrated in Figs. 2(a1) and (c1), WRF-Chem model reasonably well reproduces the spatial distribution of observed $PM_{2.5}$, with high values over large city cluster. The predicted O_3 concentrations can also reproduce the spatial variation of the observed concentrations (Figs. 2(a2) and (c2)). NO_2 is an important precursor of O_3 and aerosol, a good performance on NO_2 is necessary. From Figs. 2(a3) and (c3), the model can well reproduce the spatial distribution of observed NO_2. Although the distributions of simulated air pollutants are in good with the observations, biases still exist, which may be due to the uncertain in the emission inventories. Figures 2(b1-b3) and 2(d1-d3) show the temporal profiles of observed and simulated surface-layer air pollutants averaged over monitoring sites and the grid cell containing the monitor site in eastern China. The statistical metrics are also shown in Table 2. As shown in Figs. 2(b1) and (d1), the model tracks well with the diurnal variation of $PM_{2.5}$ over the eastern China, with R of 0.63 and 0.80, respectively. But the model slightly underestimates the concentrations of $PM_{2.5}$ with MB of -6.3 and -10.1 μg m^{-3}, respectively, in summer and winter. Simulated O_3 agree reasonably well with observations with R of 0.90 and 0.86, and small MB are found in summer and winter with values of -0.6 and 2.8 ppb, respectively. The model tracks the daily variation of observed NO_2 reasonably well, with R of 0.73 and 0.83. But the model slightly underestimates the NO_2 against measurements, with MB of -1.5 and -4.5 ppb, respectively, in summer and winter. In general, WRF-Chem model can well reproduce the features of observed meteorology and air pollutants over eastern China.

3.3 Evaluation for changes in air pollutants from 2013 to 2017

Figure 3 demonstrates the spatial distribution of changed summer (left) and winter (right) surface (a, b) $PM_{2.5}$ and (c, d) MDA8 O_3 from 2013 to 2017. As shown in Figs. 3(a) and 3(b), the observed concentrations of $PM_{2.5}$ in eastern China are significantly reduced both in summer (-16.2 μg m^{-3}) and winter (-56.0 μg m^{-3}), and these changes can be well captured by the model (-14.3 μg m^{-3} for summer and -49.8 μg m^{-3} for winter). Therefore, the model can reproduce the observed decrease in $PM_{2.5}$ levels from 2013 to 2017. As shown in Figs. 3(c) and 3(d), the model reasonably well reproduces the seasonal patterns of changed surface MDA8 O_3 over the eastern China during summer and winter from 2013 to 2017. In summer, both the observations and simulations show the increased (decreased) MDA8 O_3 in YRD (PRD and SCB), while the model can not simulate the positive changes in MDA8 O_3 over BTH, and the potential reasons may be that this study did not consider the effect of changes in aerosol heterogeneous reactions. Li et al. (2019) found that the weakened uptake of HO_2 on aerosol surfaces was the main reason for the O_3 increase over BTH. In contrast to the changes in summer, observed MDA8 O_3 in winter generally increased over the eastern China, which can be well reproduced by the model.

4. Results and Discussion

4.1 Impacts of changed meteorology and anthropogenic emission on O_3

The strategy of clean air action decreased the anthropogenic emission of NO_x, but the changes in anthropogenic VOCs emissions were unobvious (Fig. S4), which might influence the O_3 formation sensitive regime and the O_3 concentration. Figure ~~3~~ 4 shows the spatial distributions of changed summer and winter MDA8 O_3 concentrations from 2013 to 2017 ~~over eastern China, and the contributions of~~due to changed anthropogenic emissions alone and changed meteorological conditions alone. As shown in Fig. ~~3~~4(a~~b~~), the concentration of summer MDA8 O_3 from 2013 to 2017 was increased in city clusters, but it was decreased in rural regions. This discrepancy might be explained by the ozone formation regimes in urban (typically VOCs-limited) and rural (typically NO_x-limited) areas during summer (Li et al., 2019; Wang et al., 2019). Contrary to the

phenomenon in summer, decreased anthropogenic emissions lead to a uniform increase in winter MDA8 O_3 over the whole eastern China (Fig. ~~3~~4(~~e~~c)). These different spatial variation characteristics in summer and winter could be explained by the different ozone formation regimes in winter (VOCs-limited) and summer (NO_x-limited) (Fig. S5, Jin and Holloway, 2015). From Figs. ~~3~~4(~~e~~b) and (~~f~~d), the impacts of changed meteorological conditions on MDA8 O_3 varied by regions, ranging from -24.9 (-14.0) to 17.0 (7.3) ppb in summer (winter). Focusing on the four developed city clusters, compared with 2013, the meteorological conditions in the summer of 2017 promoted the generation of O_3 in the YRD region (Fig. 8(a3)), but suppressed the generation of O_3 in the BTH (Fig. 8(a2)), PRD (Fig. 8(a4)) and SCB (Fig. 8(a5)) regions. In PRD and SCB, the changes in MDA8 O_3 due to meteorology even have a greater impact than that by emission changes, which highlights the significant role of meteorology on summer O_3 variations.

~~The reductions in anthropogenic emissions from 2013 to 2017 will also lead to a decrease in $PM_{2.5}$ concentrations (Fig. S5), which can further affect the O_3 concentrations by weakened aerosol-radiation interaction (ARI). Further, we average the observed MDA8 O_3 concentrations of monitoring sites in the urban areas and the simulation value for the grid cell containing the monitoring site to examine the impacts of changed meteorological conditions, anthropogenic emissions and ARI on O_3 levels in densely populated urban areas (Fig. 4). Given that most of the monitoring stations with 5 years of continuous observations are located in urban areas. Therefore, these monitoring stations and the grid cells containing the monitoring stations can be considered as urban areas in this study (Liu and Wang, 2020b). As shown in Figs. 4(a1) and (b1), the changes in observed MDA8 O_3 over urban areas in eastern China from 2013 to 2017 can be well captured by WRF-Chem both in summer and winter. In summer, changed meteorological conditions from 2013 to 2017 has little impact on the variations in MDA8 O_3 over the urban areas, while the contribution of emission reductions to increased MDA8 O_3 is significant. In winter, changed meteorological conditions is unfavorable for the increase in MDA8 O_3 from 2013 to 2017, indicating the worsened ozone pollution driven by the changed anthropogenic emission. What's~~

~~more, the ΔO_3_ΔARI_EMI has significant effect on the increased MDA8 O_3 in summer from 2013 to 2017 with the value of +1.77 ppb (87.6%), but its impacts in winter are smaller, only +0.42 ppb (11.8%), which is consistent with the results in Li et al. (2021). Meanwhile, the contributions of ΔO_3_ΔAPI_EMI and ΔO_3_ΔARF_EMI to the increase in O_3 concentration averaged over urban areas in eastern China are almost the same in summer (0.79 vs. 0.98) and winter (0.20 vs. 0.22). The model can also capture the changes in observed summer/winter MDA8 O_3 from 2013 to 2017 over urban areas in the four city clusters (Figs. 4(a2-b5)), except BTH in summer. The reason for the underestimation over BTH may be that this study did not consider the effect of changes in aerosol heterogeneous reactions. Li et al. (2019) found that the weakened uptake of HO_2 on aerosol surfaces was the main reason for the O_3 increase over BTH. In general, we find that the enhancement of O_3 concentrations both in summer and winter is mainly caused by the factor of reduced anthropogenic emissions. Furthermore, the contributions of ΔO_3_ΔAPI_EMI and ΔO_3_ΔARF_EMI to the increases in O_3 concentrations from 2013 to 2017 over urban areas are almost the same during summer and winter.~~

4.2 Impacts of weakened aerosol-radiation interaction on O_3

Figures S6a (S7a) and S6b (S7b) present the spatial distribution of the impacts of ARF, API and ARI on surface MDA8 O_3 concentrations in summer (winter) under different anthropogenic emission conditions in year 2017 and year 2013, respectively. As shown in Fig. S6, summer MDA8 O_3 are significantly reduced over eastern China, ARF, API and ARI decrease the surface MDA8 O_3 concentrations by 0.23 (0.59) ppb, 1.09 (1.54) ppb and 1.32 (2.13) ppb under low (high) anthropogenic emission conditions in year 2017 (year 2013), respectively. The changes in MDA8 O_3 concentrations due to aerosol-radiation interaction under low emission condition are weaker than that under high emission condition. This is because the concentration of aerosols in year 2013 is higher than that in year 2017, and then its impact on meteorological conditions and J[NO_2] is greater (Fig. S8). As shown in Fig. S7a, ARF,

API and ARI decrease the winter MDA8 O_3 concentrations by 0.38 ppb (-0.9%), 1.59 ppb (-4.1%) and 1.96 ppb (-5.1%) in year 2017, respectively. Compared to the impacts under relatively high anthropogenic emission conditions in year 2013, the reduction of surface MDA8 O_3 concentrations caused by ARF, API and ARI are also greater, with the values of 0.62 ppb (-1.6%), 1.98 ppb (-5.4%) and 2.59 ppb (-7.1%), respectively. Both API and ARF reduce O_3 concentrations, and the reduction in O_3 caused by API is greater than that caused by ARF both in summer and winter.

Further, the significant reduction in $PM_{2.5}$ due to clean air action (Fig. ~~S5~~S9) will lead to an increase in O_3 concentrations as the weakened effects of aerosols on O_3. Therefore, this study further quantifies the effects of ΔO_3_Δ~~API~~ARF_EMI, ΔO_3_Δ~~ARF~~API_EMI and ΔO_3_ΔARI_EMI (ΔO_3_ΔARI_EMI = ΔO_3_ΔARF_EMI + ΔO_3_ΔAPI_EMI) on O_3 air quality. As shown in Figs. 5(a1-a3), the surface MDA8 O_3 in summer are increased over most of eastern China due to ΔO_3_Δ~~API~~ARF_EMI, ΔO_3_Δ~~ARF~~API_EMI and ΔO_3_ΔARI_EMI. The largest increases in MDA8 O_3 concentrations due to ΔO_3_Δ~~API~~ARF_EMI and ΔO_3_Δ~~ARF~~API_EMI are found in the developed four city clusters, with the increase larger than 4 ppb. Overall, ΔO_3_Δ~~API~~ARF_EMI, ΔO_3_Δ~~ARF~~API_EMI and ΔO_3_ΔARI_EMI lead to the increase in surface MDA8 O_3 by 0.36 ppb, 0.45 ppb and 0.81 ppb averaged over eastern China during summer, respectively. As shown in Fig. 5(a4-a6), the ΔO_3_Δ~~API~~ARF_EMI, ΔO_3_Δ~~ARF~~API_EMI and ΔO_3_ΔARI_EMI can also cause an increase in winter MDA8 O_3 concentrations by 0.24 ppb, 0.39 ppb and 0.63 ppb, respectively. In general, weakened aerosol-radiation interaction due to reduced anthropogenic emission from 2013 to 2017 can exacerbate ozone pollution both in summer and winter.

In order to explore the mechanism of the impacts of ΔO_3_ΔARI_EMI on MDA8 O_3, we resolve the changed O_3 into the contributions from chemical and physical processes. Figure 6 presents the accumulated changes in O_3 and each process contribution from 09:00 to 16:00 LST by the ΔO_3_ΔAPI_EMI, ΔO_3_ΔARF_EMI and ΔO_3_ΔARI_EMI ~~(ΔO_3_ΔARI_EMI=ΔO_3_ΔAPI_EMI+ΔO_3_ΔARF_EMI)~~ during summer and winter. As shown in Fig 6, the enhanced chemical production is the

dominant process leading to the increase in O_3 concentrations over eastern China and the four city clusters both in summer and winter. The leading factor of enhancement in O_3 over BTH are inconsistent with that over eastern China, and the enhancement of O_3 concentration in BTH is mainly due to ΔO_3_ΔARF_EMI. But the leading factor of enhancement in O_3 over SCB are consistent with that in eastern China, the enhancement of O_3 concentration is mainly due to ΔO_3_ΔAPI_EMI both in summer and winter. Moreover, the enhancement of O_3 concentration in BTH, YRD and PRD is mainly due to ΔO_3_ΔARF_EMI during winter, which is opposite to that of eastern China. The leading factors for the increase of O_3 concentration in different city clusters are different. The enhancement of O_3 concentration in most areas is caused by ΔO_3_ΔAPI_EMI, whereas the increase in O_3 concentration in BTH, YRD and PRD areas is dominated by ΔO_3_ΔARF_EMI in winter. In general, the weakened aerosol-radiation interaction caused by emission reduction would promote the chemical production of O_3 and increase the O_3 concentrations over eastern China in summer and winter.

In order to explore the reason for the increase in O_3 chemical production, we further analyzed the variation of HO_x ($HO+HO_2$) concentration from 2013 to 2017. As the aerosol concentration decreases, its influence on solar radiation is weakened and photolysis is enhanced, leading to an increase in HO_x levels. It can be seen from Fig. S~~9~~10 that the concentration of HO_x increases both in winter and summer. The increase in HO_x will promote the conversion of NO to NO_2, which will lead to the accumulation of O_3 concentration.

~~4.3 Impacts of weakened aerosol-radiation interaction on effectiveness of emission reduction for O_3 air quality~~

Figure 7 shows the changed summer and winter surface-layer MDA8 O_3 concentrations caused by anthropogenic emission reduction from 2013 to 2017 with (ΔO_3_EMI) and without (ΔO_3_NOARI) ARI, including the effects of weakened ARI on the effectiveness of emission reduction for O_3 air quality (ΔO_3_ΔARI_EMI, which is also equal to ΔO_3_EMI minus ΔO_3_NOARI). As shown in Figs. 7(a1) and 7(a4), the surface-layer MDA8 O_3 concentrations increased mainly in urban areas during summer and increased uniformly in winter due to anthropogenic emission reduction from 2013

to 2017 without the impact of ARI. When the effect of ARI is considered, the concentrations of MDA8 O_3 are increased more than that when ARI is not taken into account (Figs. 7(a2) and 7(a5)). The consequences of weakened ARI resulted from anthropogenic emission reduction on MDA8 O_3 concentrations are shown in Figs. 7(a3) and 7(a6). From Figs. 7(a3) and 7(a6) we can find that the concentrations of MDA8 O_3 are increased in both summer and winter over eastern China. ~~Comparing with Fig. 7(a1) and (a2) in summer and Fig. 7(a4) and (a5) in winter, when the impact of ARI is considered, the concentrations of MDA8 O_3 are increased more than that when ARI is not taken into account. Thus~~Therefore, ΔO_3_ΔARI_EMI makes the superimposed impact on the effectiveness of anthropogenic emission reduction for the increased MDA8 O_3 concentrations from 2013 to 2017 over eastern China. However, during summer, the worsened O_3 air quality due to weakened ARI can only be found in scattered city clusters (e.g., BTH, YRD and PRD in Fig. 7(a3)). During winter, it ~~would~~ will increase MDA8 O_3 concentrations over nearly the whole eastern China (Fig. 7(a6)).

We also average the observed MDA8 O_3 concentrations of monitoring sites in the urban areas and the simulation value for the grid cell containing the monitoring site to further examine the impacts of changed meteorological conditions, anthropogenic emissions and ARI on O_3 levels in densely populated urban areas (Fig. 8). Given that most of the monitoring stations with 5 years of continuous observations are located in urban areas. Therefore, these monitoring stations and the grid cells containing the monitoring stations can be considered as urban areas in this study (Liu and Wang, 2020b). As shown in Figs. 8(a1) and 8(b1), the changes in observed MDA8 O_3 over urban areas in eastern China from 2013 to 2017 can be well captured by WRF-Chem both in summer and winter. In summer, changed meteorological conditions from 2013 to 2017 has little impact on the variations in MDA8 O_3 over the urban areas, while the contribution of emission reductions to increased MDA8 O_3 is significant. In winter, changed meteorological conditions is unfavorable for the increase in MDA8 O_3 from 2013 to 2017, indicating the worsened ozone pollution driven by the changed anthropogenic emission. What's more, the ΔO_3_ΔARI_EMI has significant effect on

the increased MDA8 O_3 in summer from 2013 to 2017 with the value of +1.77 ppb (87.6%), but its impacts in winter are smaller, only +0.42 ppb (11.8%), which is consistent with the results in Li et al. (2021). The increased MDA8 O_3 concentration over urban areas in summer caused by O_3_ΔARI_EMI in this study is 1.77 ppb, which is compared to the value of 2.12 ppb increase caused by weakened aerosol heterogeneous reactions quantified by Liu and Wang (2020b). Meanwhile, the contributions of ΔO_3_ΔAPI_EMI and ΔO_3_ΔARF_EMI to the increase in O_3 concentration averaged over urban areas in eastern China are almost the same in summer (0.79 vs. 0.98) and winter (0.20 vs. 0.22). In general, we find that the enhancement of O_3 concentrations both in summer and winter is mainly caused by the factor of reduced anthropogenic emissions. Furthermore, the contributions of ΔO_3_ΔAPI_EMI and ΔO_3_ΔARF_EMI to the increases in O_3 concentrations from 2013 to 2017 over urban areas are almost the same during summer and winter.

4.3 Discussions

(1) The CBMZ gas-phase chemistry coupled with MOSAIC aerosol module (CBMZ-MOSAIC for short) used in this study does not include secondary organic aerosol (SOA), then Here we applied three additional chemical mechanisms that consider SOA, namely, RADM2 gas-phase chemistry coupled with MADE/SORGAM aerosol module (RADM2-MADE/SORGAM for short), CBMZ gas-phase chemistry coupled with MADE/SORGAM aerosol module (CBMZ-MADE/SORGAM for short), and MOZART gas-phase chemistry coupled with MOSAIC aerosol module (MOZART-MOSAIC for short), to test the impact of ARI on O_3 with and without SOA for the scenario of BASE_17E17M.

Figures S11 shows the temporal variations of observed and simulated $PM_{2.5}$ and O_3 concentrations over eastern China for the three additional chemical mechanisms. Comparing with the observed $PM_{2.5}$ (O_3) concentrations, the MOZART-MOSAIC showed the best performance in December 2017, with the R of 0.73 (0.79) and NMB of -18.7% (-20.5%). Therefore, we further used this mechanism to simulate the air

pollutant concentrations during the period of June 2017. As shown in Fig. S11 (a4, b4), the temporal variations of observed $PM_{2.5}$ (O_3) can be well captured by this mechanism with R of 0.56 (0.91) and NMB of -1.7% (-20.3%).

Finally, we investigated the effect of ARI on O_3 from the results of CBMZ-MOSAIC (this mechanism applied in this manuscript which does not include SOA) and MOZART-MOSAIC (this mechanism includes SOA and performs the best simulation results comparing with RADM2-MADE/SORGAM and CBMZ-MADE/SORGAM). As shown in Fig. S12, summer (winter) MDA8 O_3 is significantly reduced over eastern China, ARI reduces the surface MDA8 O_3 concentrations by 1.32 (1.96) ppb and 1.85 (1.60) ppb by CBMZ-MOSAIC and MOZART-MOSAIC, respectively. The O_3 reductions are of comparable magnitude in these two schemes. Therefore, we can conclude that although the CBMZ-MOSAIC applied in this manuscript does not take into account the formation of SOA and its associated effects, the aerosol radiative effects on O_3 concentrations not only in the pattern of spatial-temporal distribution but also in the order of magnitude are consistent with the results when the SOA simulation mechanism is considered.

As shown in Fig. S13, the mean SOA simulated by RADM2-MADE/SORGAM, CBMZ-MADE/SORGAM, and MOZART-MOSAIC are 0.29, 0.45 and 0.94 $\mu g\ m^{-3}$, accounting for 3.4%, 3.8%, and 4.4% of $PM_{2.5}$ concentrations in winter 2017, respectively. From Fig. S14, the mean SOA simulated from MOZART-MOSAIC is 0.90 $\mu g\ m^{-3}$, account for 9.1% of $PM_{2.5}$ in summer 2017. Model simulated SOA concentrations are generally underestimated in most current chemical transport models (Zhang et al., 2015; Zhao et al., 2015). The low SOA concentrations simulated by the model can be explained by low emissions of biogenic and anthropogenic VOCs (key precursors of SOA), but a thorough investigation of this underestimation is outside the scope of this manuscript and it will be discussed in our future work.

(2) The impacts of aerosol heterogeneous reactions (HET) on O_3 have not been considered in this manuscript due to the uncertainty and inconsistency of the heterogeneous uptake shown in previous observation and simulation studies (Liu and Wang., 2020b; Tan et al., 2020; Shao et al., 2021). Liu and Wang. (2020b) found that

the rapid decrease of $PM_{2.5}$ was the primary contributor for the summer O_3 increase through weakening the heterogeneous uptake of hydroperoxy radical (HO_2). However, Tan et al. (2020) launched a field campaign in NCP and proposed a contradicting opinion about the importance of the impact of HET on O_3. Shao et al. (2021) summarized that different heterogeneous uptake on the aerosol surface applied in the model simulation (e.g., 0.20 *vs.* 0.08) would cause significant deviations in simulated ozone concentrations (e.g., O_3 increased by 6% *vs.* O_3 increased by 2.5%). Previous laboratory studies indicate that the dependence of the uptake coefficient on aerosol composition and RH means that a single assumed value for heterogeneous uptake used in numerical simulations can lead to large uncertainties (Lakey et al., 2015; Taketani et al., 2009; Zou et al., 2019). Therefore, the uncertainty in the heterogeneous uptake value used in the numerical simulation will finally amplify the deviation in model results. Meanwhile, our manuscript devoted to quantifying the effects of ARI on O_3, rather than the impacts of heterogeneous reactions on O_3. The absence of heterogeneous chemistry on aerosol surface may result in underestimation of the effect of aerosol on O_3, which will be considered in our future work.

(3) There may be an interaction between API and ARF. However, in this study we discuss the role of API and ARF separately, which may ignore the effects of interactions between API and ARF on O_3. This may affect our results, and we will discuss their interaction in our future studies.

5 Conclusions

In this study, the impact of weakened aerosol-radiation interaction (ARI) due to decreased anthropogenic emissions on surface O_3 (ΔO_3_ΔARI_EMI) over eastern China is mainly analyzed by using an online-coupled regional chemistry transport model WRF-Chem. Simulation results generally reproduce the spatiotemporal characteristics of observations with correlation coefficients of 0.63-0.90 for pollutant concentrations and 0.40-0.99 for meteorological parameters, respectively.

Sensitivity experiments show that the changes in MDA8 O_3 from 2013 to 2017 over eastern China vary spatially and seasonally, and the decreased anthropogenic

emission plays a more prominent role for the MDA8 O_3 increase than the impact of changed meteorological conditions both in summer and winter. Furthermore, the decreased $PM_{2.5}$ concentrations due to reduced anthropogenic emissions can result in a weaker impact of ARI on O_3 concentrations, which finally pose a superimposed effect on the worsened O_3 air quality. For urban areas over eastern China, ΔO_3_ΔARI_EMI has a significant effect on the increase of MDA8 O_3 in summer with the value of +1.77 ppb, accounting for 87.6% of the increased value caused by decreased anthropogenic emissions, but the impacts in winter are smaller (+0.42 ppb), accounting for 11.8% of the increased value caused by decreased anthropogenic emissions. For the whole regions over eastern China, the enhancement of MDA8 O_3 by ΔO_3_ΔARI_EMI is +0.81 (+0.63) ppb, with ΔO_3_ΔAPI_EMI and ΔO_3_ΔARF_EMI contributing for 55.6% (61.9%) and 44.4% (38.1%) in summer (winter), respectively. Process analysis shows that the enhanced O_3 chemical production is the dominant process for the increased O_3 concentrations caused by ΔO_3_ΔARI_EMI both in summer and winter.

Generally, since China's clean air action from 2013, the decreased $PM_{2.5}$ concentrations due to reduced anthropogenic emissions can worsen O_3 air quality by the weakened interactions between aerosol and radiation, which is a new and an important implication for understanding the causes driving the increases in O_3 level over eastern China. Therefore, our results highlight that more carefully designed multi-pollutants coordinated emissions control strategies are needed to reduce the concentrations of $PM_{2.5}$ and O_3 simultaneously.

Data availability

The observed hourly surface concentrations of air pollutants are derived from the China National Environmental Monitoring Center (http://www.cnemc.cn). The observed surface meteorological data are obtained from NOAA's National Climatic Data Center (https://gis.ncdc.noaa.gov/maps/ncei/cdo/hourly). The photolysis rates of nitrogen dioxide in Beijing are provided by Xin Li (li_xin@pku.edu.cn). The simulation results can be accessed by contacting Lei Chen (chenlei@nuist.edu.cn) and Hong Liao (hongliao@nuist.edu.cn).

Author contributions

HY, LC, and HL conceived the study and designed the experiments. HY and LC performed the simulations and carried out the data analysis. JZ, WW, and XL provided useful comments on the paper. HY prepared the paper with contributions from all co-authors.

Competing interests

The authors declare that they have no competing interests.

Acknowledgements

This work is supported by National Natural Science Foundation of China (Grant 42305121, 42007195, 42293320), National Key R&D Program of China (Grant 2019YFA0606804, 2022YFE0136100), and Natural Science Foundation of Jiangsu Province (Grant BK20220031), Guizhou Provincial Science and Technology Projects of China (CXTD [2022]001, GCC [2023]026), and Open fund by Jiangsu Key Laboratory of Atmospheric Environment Monitoring and Pollution Control (KHK 2211).

Reference

Atkinson, R.: Atmospheric chemistry of VOCs and NOx, Atmos Environ., 34, 2063–2101, https://doi.org/10.1016/S1352-2310(99)00460-4, 2000.

~~Barnard, J. C., Fast, J. D., Paredes-Miranda, G., Arnott, W. P., and Laskin, A.: Technical Note: Evaluation of the WRF-Chem "Aerosol Chemical to Aerosol Optical Properties" Module using data from the MILAGRO campaign, Atmos. Chem. Phys., 10, 7325–7340, https://doi.org/10.5194/acp-10-7325-2010, 2010.~~

Chen, F. and Dudhia, J.: Coupling an Advanced Land Surface – Hydrology Model with the Penn State – NCAR MM5 Modeling System. Part I: Model Implementation and Sensitivity, Mon. Weather Rev., 129(4), 569–585, 2001.

Cheng, Y., Zheng, G., Chao, W., Mu, Q., Bo, Z., Wang, Z., Meng, G., Qiang, Z., He, K., and Carmichael, G.: Reactive nitrogen chemistry in aerosol water as a source of sulfate during haze events in China, Science Advances, 2, https://doi.org/10.1126/sciadv.1601530, 2016.

Dang, R. and Liao, H.: Radiative Forcing and Health Impact of Aerosols and Ozone in China as the Consequence of Clean Air Actions over 2012–2017, Geophys. Res. Lett., 46, 12511–12519, https://doi.org/10.1029/2019GL084605, 2019.

~~Dickerson, R. R., Kondragunta, S., Stenchikov, G., Civerolo, K. L., Doddridge, B. G., and Holben, B. N.: The impact of aerosols on solar ultraviolet radiation and photochemical smog, Science, 278, 827-830, 10.1126/science.278.5339.827, 1997.~~

Foken, T.: 50 years of the Monin-Obukhov similarity theory, Bound.-Layer Meteor., 119, 431–437, 2006.

Gipson, G. L.: Science algorithms of the EPA Models-3 community multiscale air quality (CMAQ) modeling system: Chapter 16, process analysis, edited by: Byun, D. W. and Ching, J. K. S., Reported No. EPA/600/R-99/030, U.S. Environmental Protection Agency, Office of Research and Development, Washington, D.C., 1999.

Grell G A.: Prognostic evaluation of assumptions used by cumulus parameterizations, Monthly Weather Review., 121, 764–787, 1993.

Grell, G. A., Peckham, S. E., Schmitz, R., Mckeen, S. A., Frost, G., Skamarock, K.,

and Eder, B.: Fully coupled “online” chemistry within the WRF model, Atmos. Environ., 39, 6957–6975, 2005.

Guenther, A., Karl, T., Harley, P., Wiedinmyer, C., Palmer, P. I., and Geron, C.: Estimates of global terrestrial isoprene emissions using MEGAN (Model of Emissions of Gases and Aerosols from Nature), Atmos. Chem. Phys., 6, 3181–3210, doi:10.5194/acp-6-3181-2006, 2006.

Hong, C., Zhang, Q., Zhang, Y., Davis, S. J., Zhang, X., Tong, D., Guan, D., Liu, Z., and He, K.: Weakening aerosol direct radiative effects mitigate climate penalty on Chinese air quality, Nat. Clim. Change, 10, 845–850, https://doi.org/10.1038/s41558-020-0840-y, 2020.

Hong, S.-Y., Noh, Y., and Dudhia, J.: A New Vertical Diffusion Package with an Explicit Treatment of Entrainment Processes, Mon. Weather Rev., 134, 2318–2341, 2006.

Iacono, M. J., Delamere, J. S., Mlawer, E. J., Shephard, M. W., Clough, S. A., and Collins, W. D.: Radiative forcing by long-lived greenhouse gases: Calculations with the AER radiative transfer models, J. Geophys. Res., 113, D13103, doi:10.1029/2008JD009944, 2008.

~~Jacob, D. J.: Heterogeneous chemistry and tropospheric ozone, Atmos. Environ., 34, 2131–2159, doi:10.1016/S1352-2310(99)00462-8, 2000.~~

Jimenez, P. A. and Dudhia, J.: Improving the representation of resolved and unresolved topographic effects on surface wind in the WRF model, J. Appl. Meteorol. Clim., 51, 300–316, 2012.

Jin, X. and Holloway, T.: Spatial and temporal variability of ozone sensitivity over China observed from the Ozone Monitoring Instrument, J. Geophys. Res.-Atmos., 120, 7229–7246, https://doi.org/10.1002/2015JD023250, 2015.

Lakey, P. S. J., George, I. J., Whalley, L. K., Baeza-Romero, M. T., and Heard, D. E.: Measurements of the HO_2 Uptake Coefficients onto Single Component Organic Aerosols, Environmental Science & Technology, 49, 4878-4885, 10.1021/acs.est.5b00948, 2015.

Lelieveld, J., Evans, J. S., Fnais, M., Giannadaki, D., and Pozzer, A.: The contribution of outdoor air pollution sources to premature mortality on a global scale, Nature, 525, 367–371, https://doi.org/10.1038/nature15371, 2015.

Li, K., Jacob, D. J., Liao, H., Qiu, Y. L., Shen, L., Zhai, S. X., Bates, K. H., Sulprizio, M. P., Song, S. J., Lu, X., Zhang, Q., Zheng, B., Zhang, Y. L., Zhang, J. Q., Lee, H. C., and Kuk, K. S.: Ozone pollution in the North China Plain spreading into the late-winter haze season, 118, P. Natl. Acad. Sci. USA, https://doi.org/10.1073/pnas.2015797118, 2021.

Li, K., Jacob, D. J., Liao, H., Shen, L., Zhang, Q., and Bates, K. H.: Anthropogenic Drivers of 2013–2017 Trends in Summer Surface Ozone in China, P. Natl. Acad. Sci. USA, 116, 422–427, https://doi.org/10.1073/pnas.1812168116, 2019.

Li, K., Jacob, D. J., Shen, L., Lu, X., De Smedt, I., and Liao, H.: Increases in surface ozone pollution in China from 2013 to 2019: anthropogenic and meteorological influences, Atmos. Chem. Phys., 20, 11423–11433, https://doi.org/10.5194/acp-20-11423-2020, 2020.

Liao, H., Yung, Y. L., and Seinfeld, J. H.: Effects of aerosols on tropospheric photolysis rates in clear and cloudy atmospheres, J. Geophys. Res., 104, 23697–23707, 1999.

Lin, Y.-L., Farley, R. D., and Orville, H. D.: Bulk parameterization of the snow field in a cloud model, J. Clim. Appl. Meteorol., 22, 1065–1092, 1983.

Liu, Y. and Wang, T.: Worsening urban ozone pollution in China from 2013 to 2017 – Part 1: The complex and varying roles of meteorology, Atmos. Chem. Phys., 20, 6305–6321, https://doi.org/10.5194/acp-20-6305-2020, 2020a.

Liu, Y. and Wang, T.: Worsening urban ozone pollution in China from 2013 to 2017 – Part 2: The effects of emission changes and implications for multi-pollutant control, Atmos. Chem. Phys., 20, 6323–6337, https://doi.org/10.5194/acp-20-6323-2020, 2020b.

Lou, S., Liao, H., and Zhu, B.: Impacts of aerosols on surface-layer ozone concentrations in China through heterogeneous reactions and changes in photolysis rates, Atmos. Environ., 85, 123–138, 2014.

Lu, X., Hong, J. Y., Zhang, L., Cooper, O. R., Schultz, M. G., Xu, X. B., Wang, T.,

Gao, M., Zhao, Y. H., and Zhang, Y. H.: Severe surface ozone pollution in China: A global perspective, Environ. Sci. Tech. Lett., 5, 487–494, https://doi.org/10.1021/acs.estlett.8b00366, 2018.

Mills, G., Sharps, K., Simpson, D., Pleijel, H., Broberg, M., Uddling, J., Jaramillo, F., Davies, W. J., Dentener, F., Van den Berg, M., Agrawal, M., Agrawal, S. B., Ainsworth, E. A., Buker, P., Emberson, L., Feng, Z., Harmens, H., Hayes, F., Kobayashi, K., Paoletti, E., and Van Dingenen, R.: Ozone pollution will compromise efforts to increase global wheat production, Glob. Change Biol., 24, 3560–3574, https://doi.org/10.1111/gcb.14157, 2018.

Seinfeld, J. H. and Pandis, S. N.: Atmospheric Chemistry and Physics: from Air Pollution to Climate Change, second ed., John Wiley and Sons, 2006.

Shao, M., Wang, W. J., Yuan, B., Parrish, D. D., Li, X., Lu, K. D., Wu, L. L., Wang, X. M., Mo, Z. W., Yang, S. X., Peng, Y. W., Kuang, Y., Chen, W. H., Hu, M., Zeng, L. M., Su, H., Cheng, Y. F., Zheng, J. Y., Zhang, Y. H.: Quantifying the role of $PM_{2.5}$ dropping in variations of ground-level ozone: Inter-comparison between Beijing and Los Angeles, Sci. Total Environ., https://doi.org/10.1016/j.scitotenv.2021.147712, 2021.

Shu, L., Wang, T., Han, H., Xie, M., Chen, P., Li, M., and Wu, H.: Summertime ozone pollution in the Yangtze River Delta of eastern China during 2013–2017: Synoptic impacts and source apportionment, Environ. Pollut., 257, 113631, https://doi.org/10.1016/j.envpol.2019.113631, 2020.

Shu, L., Xie, M., Wang, T., Gao, D., Chen, P., Han, Y., Li, S., Zhuang, B., and Li, M.: Integrated studies of a regional ozone pollution synthetically affected by subtropical high and typhoon system in the Yangtze River Delta region, China, Atmos. Chem. Phys., 16, 15801–15819, https://doi.org/10.5194/acp-16-15801- 2016, 2016.

Skamarock, W., Klemp, J. B., Dudhia, J., Gill, D. O., Barker, D. M., Duda, M., Huang, X. Y., Wang,W., and Powers, J. G.: A description of the advanced research WRF version 3, NCAR technical note NCAR/TN/u2013475, 2008.

Taketani, F., Kanaya, Y., and Akimoto, H.: Heterogeneous loss of HO_2 by KCl, synthetic sea salt, and natural seawater aerosol particles, Atmospheric Environment,

43, 1660-1665, 2009.

Tan Z, Hofzumahaus A, Lu K, Brown SS, Holland F, Huey LG, et al. No Evidence for a Significant Impact of Heterogeneous Chemistry on Radical Concentrations in the North China Plain in Summer 2014. Environ. Sci. Technolc. 54, 5973-5979, 2020.

Wang, J., Allen, D. J., Pickering, K. E., Li, Z., and He, H.: Impact of aerosol direct effect on East Asian air quality during the EAST-AIRE campaign, J. Geophys. Res.-Atmos., 121, https://doi.org/10.13016/M27W0S, 2016.

~~Wang, K., Zhang, Y., Nenes, A., and Fountoukis, C.: Implementation of dust emission and chemistry into the Community Multiscale Air Quality modeling system and initial application to an Asian dust storm episode, Atmos. Chem. Phys., 12, 10209-10237, doi:10.5194/acp-12-10209-2012, 2012.~~

Wang, N., Lyu, X., Deng, X., Huang, X., Jiang, F., and Ding, A.: Aggravating O3 pollution due to NOx emission control in eastern China, Sci. Total Environ., 677, 732–744, 2019.

Wild, O., Zhu, X., and Prather, M. J.: Fast-J: Accurate simulation of in- and below-cloud photolysis in tropospheric chemical models, J. Atmos. Chem., 37, 245–282, doi:10.1023/A:1006415919030, 2000.

Yang, H., Chen, L., Liao, H., Zhu, J., Wang, W., and Li, X.: Impacts of aerosol–photolysis interaction and aerosol–radiation feedback on surface-layer ozone in North China during multi-pollutant air pollution episodes, Atmos. Chem. Phys., 22, 4101–4116, https://doi.org/10.5194/acp-22-4101-2022, 2022.

Yue, X., Unger, N., Harper, K., Xia, X., Liao, H., Zhu, T., Xiao, J., Feng, Z., and Li, J.: Ozone and haze pollution weakens net primary productivity in China, Atmos. Chem. Phys., 17, 6073–6089, https://doi.org/10.5194/acp-17-6073-2017, 2017.

Zaveri, R. A. and Peters, L. K.: A new lumped structure photochemical mechanism for large-scale applications, J. Geophys. Res., 104, D23, 30387–30415, https://doi.org/10.1029/1999JD900876, 1999.

Zaveri, R. A., Easter, R. C., Fast, J. D., and Peters, L. K.: Model for simulating aerosol interactions and chemistry (MOSAIC), J. Geophys. Res., 113, D13204, https://doi.org/10.1029/2007JD008782, 2008.

Zhai, S., Jacob, D. J., Wang, X., Shen, L., Li, K., Zhang, Y., Gui, K., Zhao, T., and Liao, H.: Fine particulate matter (PM2.5) trends in China, 2013–2018: separating contributions from anthropogenic emissions and meteorology, Atmos. Chem. Phys., 19, 11031–11041, https://doi.org/10.5194/acp-19-11031-2019, 2019.

Zhang, B., Wang, Y., and Hao, J.: Simulating aerosol–radiation–cloud feedbacks on meteorology and air quality over eastern China under severe haze conditions in winter, Atmos. Chem. Phys., 15, 2387–2404, https://doi.org/10.5194/acp-15-2387-2015, 2015.

Zhang, Q., Zheng, Y., Tong, D., Shao, M., Wang, S., Zhang, Y., Xu, X., Wang, J., He, H., Liu, W., Ding, Y., Lei, Y., Li, J., Wang, Z., Zhang, X., Wang, Y., Cheng, J., Liu, Y., Shi, Q., Yan, L., Geng, G., Hong, C., Li, M., Liu, F., Zheng, B., Cao, J., Ding, A., Gao, J., Fu, Q., Huo, J., Liu, B., Liu, Z., Yang, F., He, K., and Hao, J.: Drivers of Improved PM2.5 Air Quality in China from 2013 to 2017, P. Natl. Acad. Sci. USA, 116, 24463–24469, https://doi.org/10.1073/pnas.1907956116, 2019.

~~Zhang, Y. and Carmichael, G. R.: The Role of Mineral Aerosol in Tropospheric Chemistry in East Asia—A Model Study, J. Appl. Meteorol., 38, 353–366, doi:10.1175/1520-0450(1999)0382.0.co;2, 1999.~~

Zhao, B., Wang, S., Donahue, N. M., Chuang, W., Ruiz, L. H., Ng, N. L., Wang, Y., and Hao, J.: Evaluation of One-Dimensional and Two-Dimensional Volatility Basis Sets in Simulating the Aging of Secondary Organic Aerosol with Smog-Chamber Experiments, Environ. Sci. Technol., 49, 2245–2254, doi:10.1021/es5048914, 2015.

Zheng, B., Tong, D., Li, M., Liu, F., Hong, C., Geng, G., Li, H., Li, X., Peng, L., Qi, J., Yan, L., Zhang, Y., Zhao, H., Zheng, Y., He, K., and Zhang, Q.: Trends in China's anthropogenic emissions since 2010 as the consequence of clean air actions, Atmos. Chem. Phys., 18, 14095–14111, https://doi.org/10.5194/acp-18-14095-2018, 2018.

Zheng, B., Zhang, Q., Zhang, Y., He, K. B., Wang, K., Zheng, G. J., Duan, F. K., Ma, Y. L., and Kimoto, T.: Heterogeneous chemistry: a mechanism missing in current models to explain secondary inorganic aerosol formation during the January 2013 haze episode in North China, Atmos. Chem. Phys., 15, 2031–2049, https://doi.org/10.5194/acp-15-2031-2015, 2015.

Zhu, J., Chen, L., Liao, H., Yang, H., Yang, Y., and Yue, X.: Enhanced PM2.5 Decreases and O3 Increases in China During COVID-19 Lockdown by Aerosol-Radiation Feedback, Geophys. Res. Lett., 48, https://doi.org/10.1029/2020GL090260, 2021.

Zou Q, Song H, Tang M, Lu K. Measurements of HO_2 uptake coefficient on aqueous $(NH_4)_2SO_4$ aerosol using aerosol flow tube with LIF system. Chinese Chemical Letters. 30, 2236-2240, 2019.

Table 1. Descriptions of model sensitivity experiments.

Cases	Anthropogenic emission	Meteorological field	API[a]	ARF[a]
BASE_17E17M	2017	2017	On	On
BASE_13E13M	2013	2013	On	On
NOAPI_17E17M	2017	2017	Off	On
NOALL_17E17M	2017	2017	Off	Off
BASE_13E17M	2013	2017	On	On
NOAPI_13E17M	2013	2017	Off	On
NOALL_13E17M	2013	2017	Off	Off

[a]API means aerosol-photolysis interaction, ARF means aerosol-radiation feedback.

Table 2. Statistical parameters of the simulated 2 m temperature (T_2, k), 2 m relative humidity (RH_2, %), 10 m wind speed (WS_{10}, m s^{-1}), 10 m wind direction (WD_{10}, °), photolysis rate of NO_2 ($J[NO_2]$, 10^{-3} s^{-1}), $PM_{2.5}$ (μg m^{-3}), O_3 (ppb), and NO_2 (ppb) against observations during summer and winter in 2017. There are 1296 air pollutant monitoring stations and 353 meteorological stations.

	Summer						Winter					
Variable	**O**[a]	**M**[a]	**R**[b]	**MB**[c]	**NMB**[d] **(%)**	**RMSE**[e]	**O**[a]	**M**[a]	**R**[b]	**MB**[c]	**NMB**[d] **(%)**	**RMSE**[e]
T_2	295.3	294.2	0.99	-1.0	-3.2	1.0	275.0	272.8	0.92	-2.0	-74.1	2.5
RH_2	68.1	71.0	0.97	2.2	3.2	3.6	58.1	60.6	0.87	2.1	3.5	6.5
WS_{10}	2.6	4.2	0.77	1.6	61.6	1.6	2.6	4.7	0.82	2.1	83.2	2.1
WD_{10}	175.7	170.9	0.40	-4.6	-2.6	16.9	192.6	184.6	0.69	-7.5	-3.9	17.4
$J[NO_2]$	2.6	2.7	0.93	0.1	4.8	1.2	1.0	1.2	0.94	0.1	12.3	0.6
$PM_{2.5}$	31.0	24.8	0.63	-6.3	-20.2	8.3	69.0	58.9	0.80	-10.1	-14.6	15.6
O_3	39.7	38.9	0.90	-0.6	-1.6	6.9	17.7	20.5	0.86	2.8	15.7	5.0
NO_2	12.7	11.2	0.73	-1.5	-12.0	4.5	23.3	18.7	0.83	-4.5	-19.4	5.6

[a]***O*** and ***M*** are the averages for observed and simulated results, respectively. $O = \frac{1}{n} \times \sum_{i=1}^{n} O_i$, $M = \frac{1}{n} \times \sum_{i=1}^{n} M_i$.

[b]***R*** is the correlation coefficient between observations and model results. $R = \frac{\sum_{i=1}^{n} |(O_i - O) \times (M_i - M)|}{\sqrt{\sum_{i=1}^{n} (O_i - O)^2 + \sum_{i=1}^{n} (M_i - M)^2}}$.

[c]***MB*** is the mean bias between observations and model results. $MB = \frac{1}{n} \times \sum_{i=1}^{n} (M_i - O_i)$.

[d]***NMB*** is the normalized mean bias between observations and model results. $NMB = \frac{1}{n} \times \sum_{i=1}^{n} \frac{M_i - O_i}{O_i} \times 100\%$.

[e]***RMSE*** is the root-mean-square error of observations and model results. $RMSE = \sqrt{\frac{1}{n} \times \sum_{i=1}^{n} (M_i - O_i)^2}$.

In the above O_i and M_i are the hourly observed and simulated data, respectively, and n is the total number of hours.

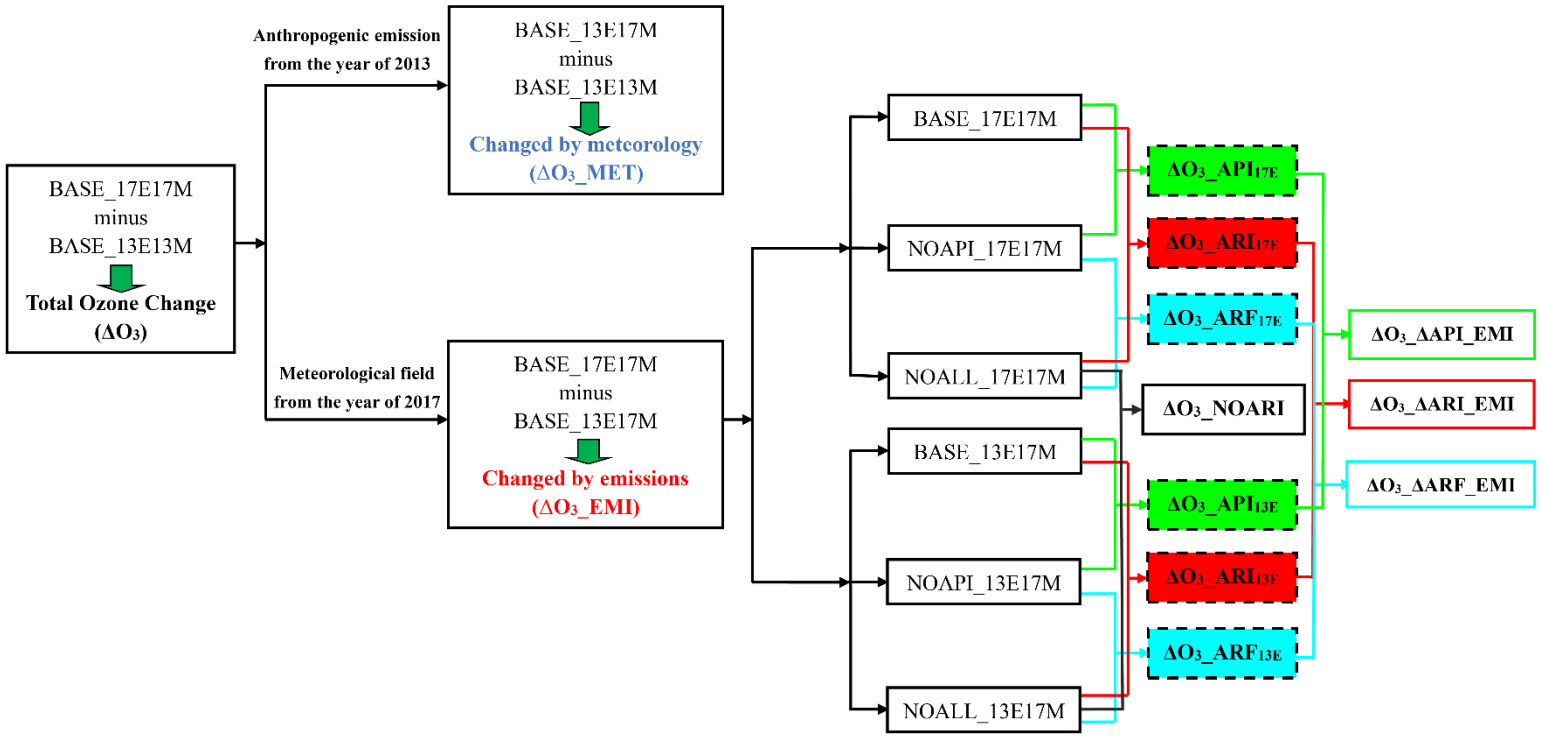

Figure 1. Schematic overview of numerical experiments. 17E17M (13E13M) means meteorological fields and anthropogenic emissions are ~~fixed~~ from the ~~at~~ year of 2017 (2013). 13E17M means anthropogenic emissions are from the year of~~fixed at year~~ 2013 but meteorological fields are at year 2017. ΔO_3_MET, ΔO_3_EMI and ΔO_3 mean the impacts of changed meteorological conditions, changed anthropogenic emissions and their combined effects on O_3, respectively. ΔO_3_API$_{17E(13E)}$, ΔO_3_ARF$_{17E(13E)}$ and ΔO_3_ARI$_{17E(13E)}$ mean the impacts of aerosol-photolysis interaction, aerosol-radiation feedback and aerosol-radiation interaction on O_3 under different emission conditions, respectively. ΔO_3_NOARI means the changed O_3 concentration by reduced anthropogenic emissions without considering aerosol-radiation interaction. ΔO_3_ΔAPI_EMI, ΔO_3_ΔARF_EMI and ΔO_3_ΔARI_EMI represent the impacts of weakened aerosol-photolysis interaction, aerosol-radiation feedback and aerosol-radiation interaction due to decreased anthropogenic emission on O_3 concentration, respectively.

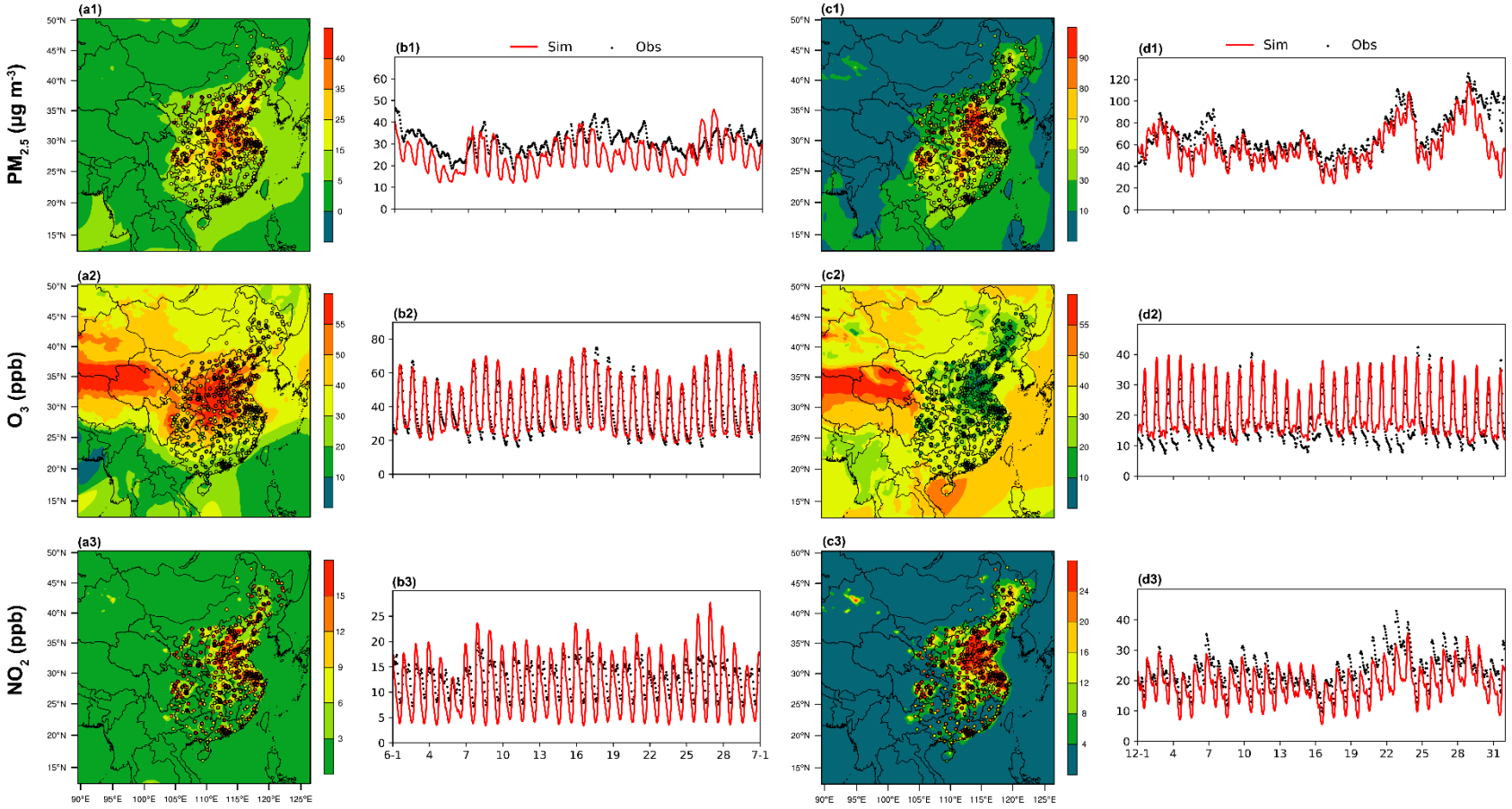

Figure 2. Spatial distributions of observed (circle) and simulated (shade) $PM_{2.5}$, O_3 and NO_2 concentrations averaged over (**a1-a3**) summer and (**c1-c3**) winter in 2017. Time series of observed (black dots) and simulated (red lines) hourly $PM_{2.5}$, O_3 and NO_2 concentrations averaged over the whole observation sites in eastern China during (**b1-b3**) summer and (**d1-d3**) winter in 2017.

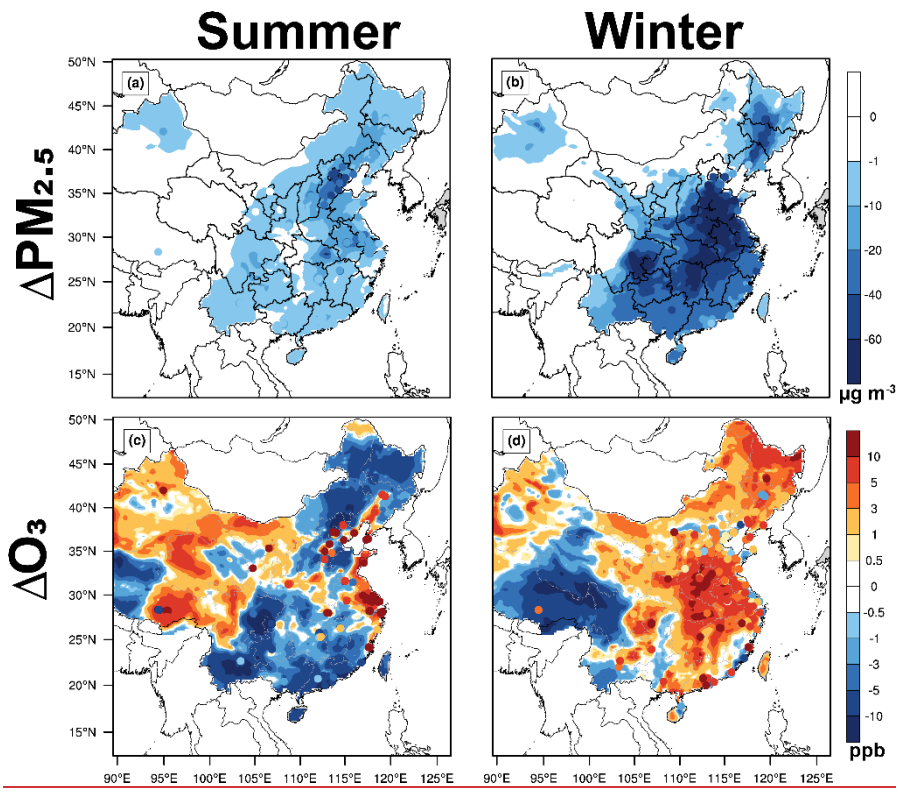

Figure 3. Spatial distribution of changed summer (left) and winter (right) surface **(a, b)** $PM_{2.5}$ and **(c, d)** MDA8 O_3 from 2013 to 2017. Observed changes in surface $PM_{2.5}$ MDA8 O_3 are also marked with colored circles. ~~**(a, d)** Spatial distribution of changed summer (upper) and winter (bottom) surface layer MDA8 O_3 from 2013 to 2017, and the contributions of **(b, e)** changed anthropogenic emissions alone and **(c, f)** changed meteorological fields alone. The observed changes in surface MDA8 O_3 are also marked with colored circles in **(a)** and **(d)**. The enclosed black line in **(f)** represents eastern China.~~

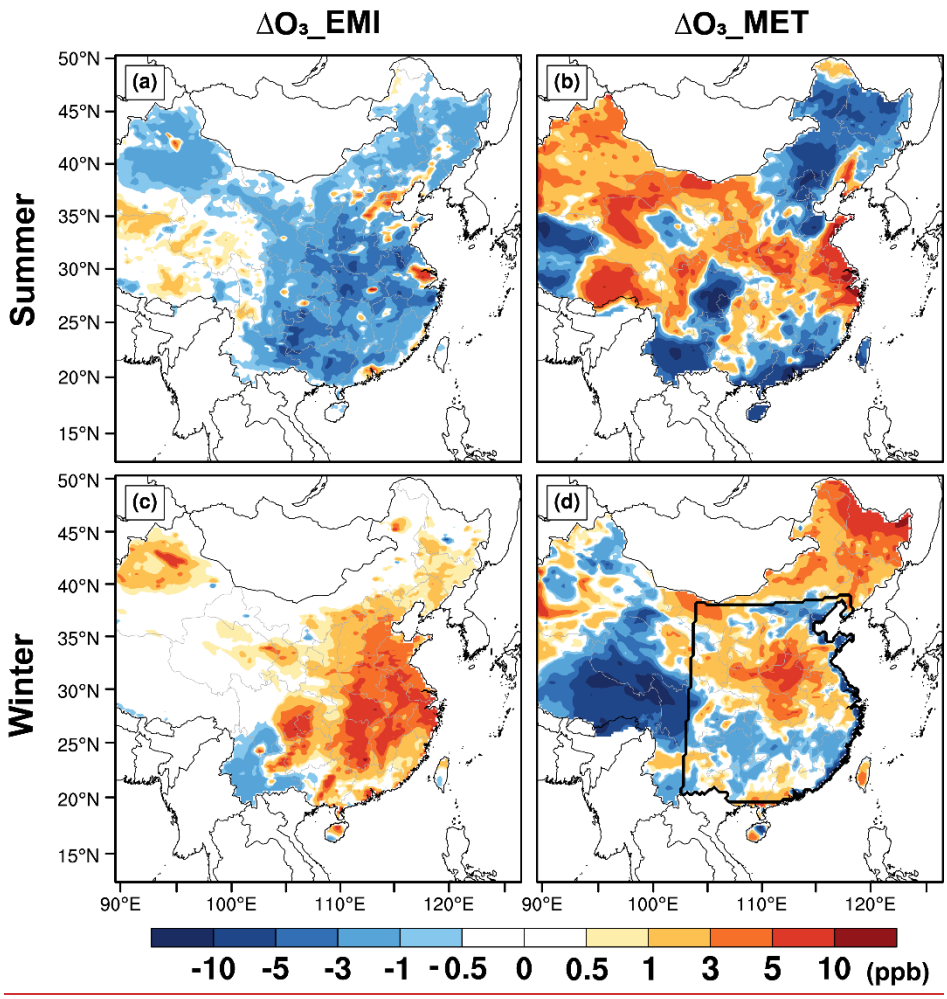

Figure 4. Spatial distribution of changed summer (upper) and winter (bottom) surface-layer MDA8 O_3 from 2013 to 2017 due to **(a, c)** changed anthropogenic emissions alone and **(b, d)** changed meteorological fields alone. The enclosed black line in **(d)** represents eastern China.

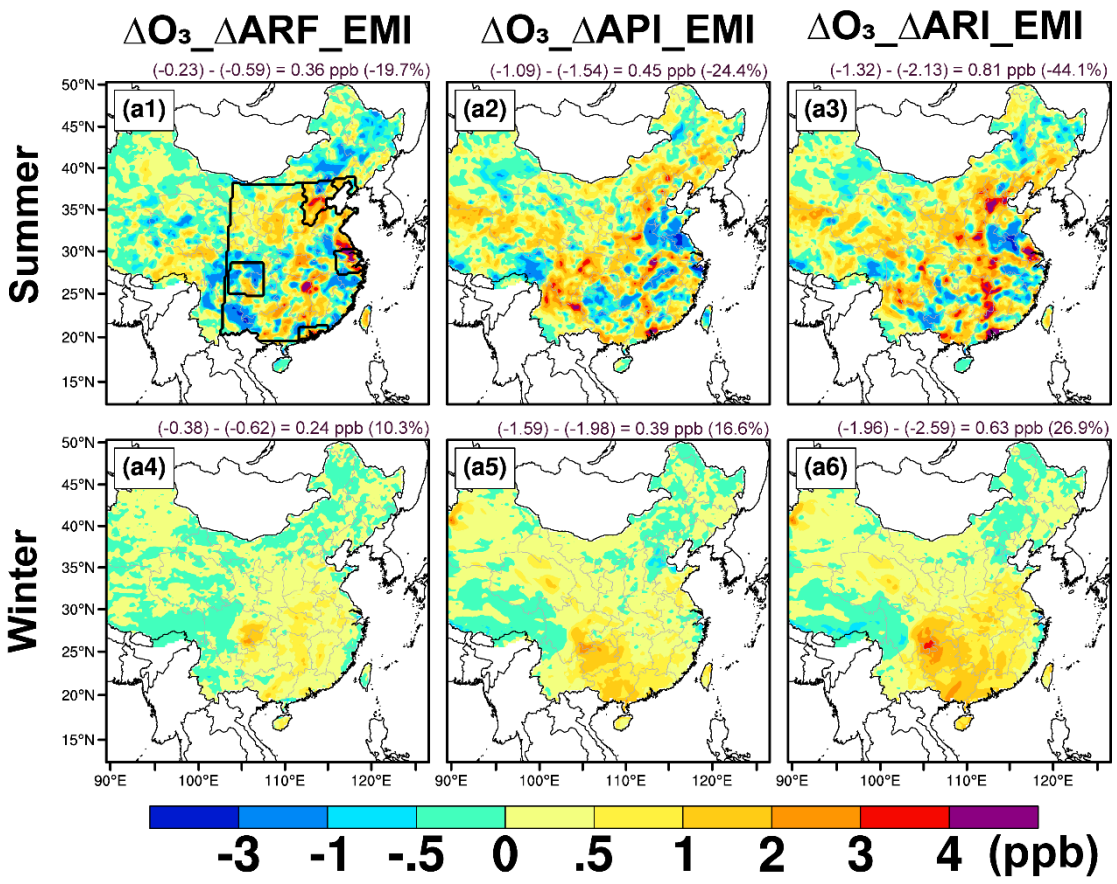

Figure 5. Impacts of ΔO_3_ΔARF_EMI, ΔO_3_ΔAPI_EMI, and ΔO_3_ΔARI_EMI on summer (upper) and winter (bottom) surface-layer MDA8 O_3 concentrations. The enclosed black line in **(a1)** represents eastern China and the four developed city clusters. The mean changes over eastern China are also shown at the top of each panel. Detailed information about ΔO_3_ΔARF_EMI, ΔO_3_ΔAPI_EMI, and ΔO_3_ΔARI_EMI can be found in Figure 1.

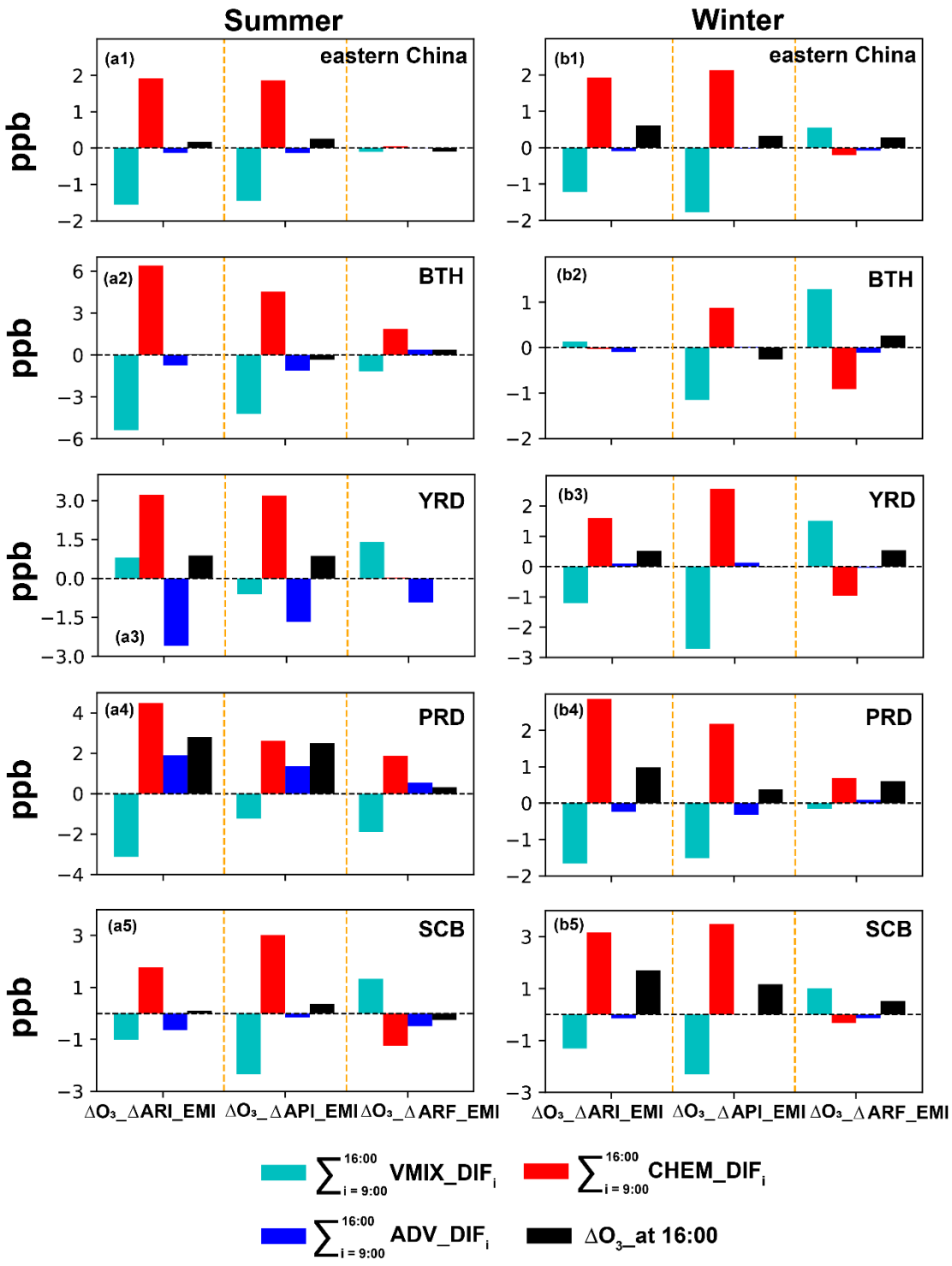

Figure 6. Accumulated changes in each process from 09:00 to 16:00 LST and the changed O_3 concentrations due to ΔO_3_ΔARI_EMI in summer (left column) and winter (right column). The regions of eastern China, Beijing-Tianjin-Hebei (BTH), Yangtze River Delta (YRD), Pearl River Delta (PRD) and Sichuan Basin (SCB) are indicated on the upper right side of each panel.

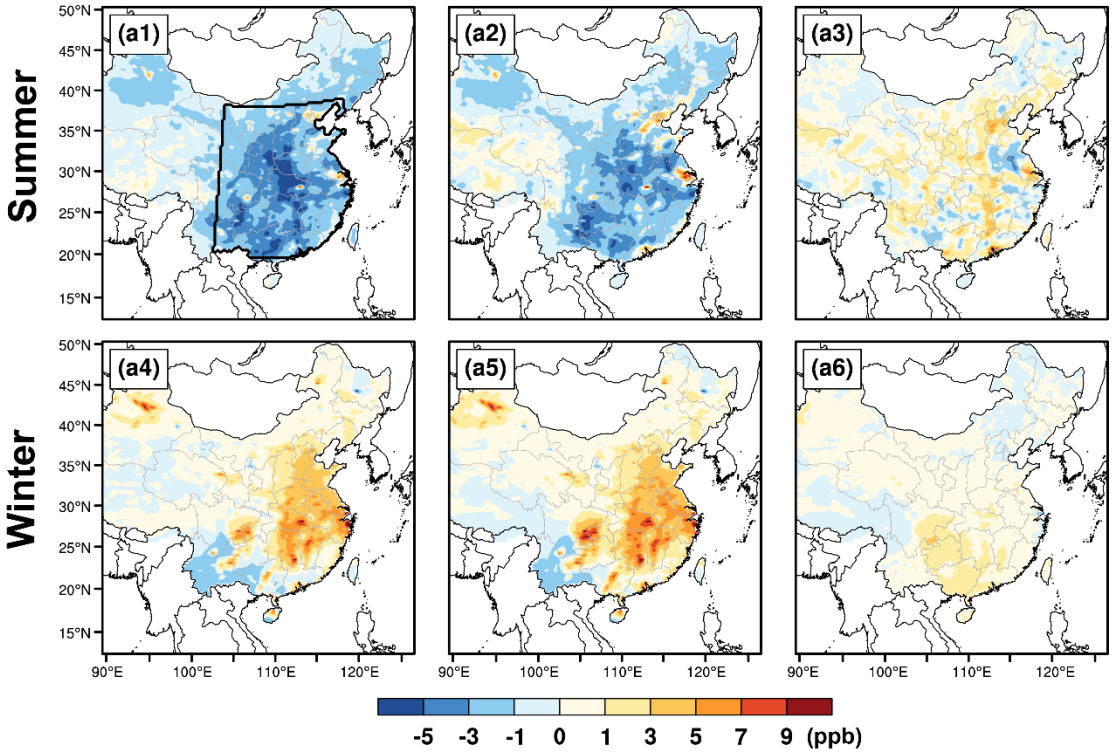

Figure 7. Spatial distribution of changed summer (upper) and winter (bottom) surface-layer MDA8 O_3 concentrations from sensitivity simulations. **(a1, a4)** Effects of anthropogenic emission reduction on MDA8 O_3 without ARI. **(a2, a5)** Effects of anthropogenic emission reduction on MDA8 O_3 with ARI. **(a3, a6)** Effects of weakened ARI on the effectiveness of emission reduction for O_3 air quality.

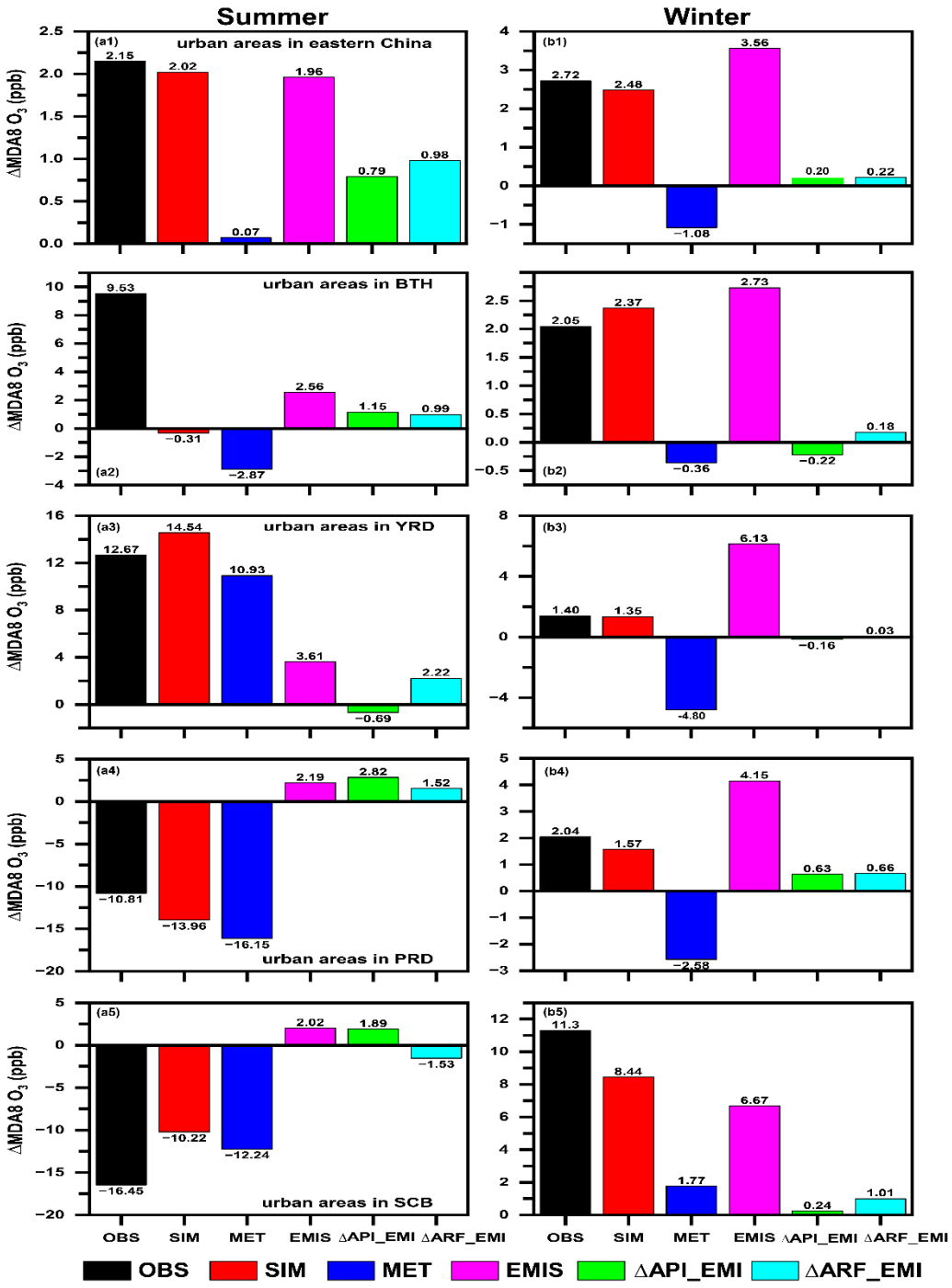

Figure 8. The observed (OBS, black bars) and simulated (SIM, red bars) changes in (left) summer and (right) winter surface-layer MDA8 O_3 from 2013 to 2017. Contributions of changed meteorological conditions alone (MET, blue bars), changed anthropogenic emissions alone (EMI, purple bars), changed aerosol-photolysis interaction alone (ΔAPI_EMI, green bars), and changed aerosol-radiation feedback alone (ΔARF_EMI, cyan bars) are also shown. Observations are calculated from the monitoring sites in the analyzed region, while the corresponding gridded simulations are averaged for SIM. **(a1-b1)**, **(a2-b2)**, **(a3-b3)**, **(a4-b4)** and **(a5-b5)** represent the urban areas in eastern China, Beijing-Tianjin-Hebei (BTH), Yangtze River Delta (YRD), Pearl River Delta (PRD), and Sichuan Basin (SCB), respectively.